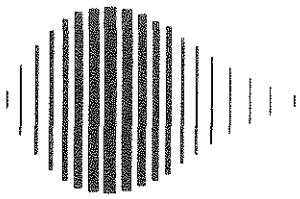

NATIONAL CENTER FOR EARTHQUAKE
ENGINEERING RESEARCH
State University of New York at Buffalo

A RESPONSE SPECTRUM APPROACH FOR ANALYSIS OF NONCLASSICALLY DAMPED STRUCTURES

by

J.N. Yang, S. Sarkani and F.X. Long
Department of Civil, Mechanical and Environmental Engineering
The George Washington University
Washington D.C. 20052

Technical Report NCEER-88-0020

April 22, 1988

This research was conducted at The George Washington University and was partially supported by the National Science Foundation under Grant No. ECE 86-07591.

NOTICE

This report was prepared by The George Washington University as a result of research sponsored by the National Center for Earthquake Engineering Research (NCEER) and the National Science Foundation. Neither NCEER, associates of NCEER, its sponsors, The George Washington University, nor any person acting on their behalf:

a. makes any warranty, express or implied, with respect to the use of any information, apparatus, method, or process disclosed in this report or that such use may not infringe upon privately owned rights; or

b. assumes any liabilities of whatsoever kind with respect to the use of, or for damages resulting from the use of, any information, apparatus, method or process disclosed in this report.

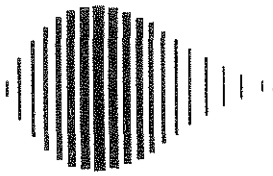

A RESPONSE SPECTRUM APPROACH FOR ANALYSIS OF NONCLASSICALLY DAMPED STRUCTURES

by

J.N. Yang[1], S. Sarkani[2] and F.X. Long[3]

April 22, 1988

Technical Report NCEER-88-0020

NCEER Contract Number 87-2004

NSF Master Contract Number ECE 86-07591

1 Professor, Dept. of Civil, Mechanical and Environmental Engineering, The George Washington University

2 Assistant Professor, Dept. of Civil, Mechanical and Environmental Engineering, The George Washington University

3 Visiting Scholar, Dept. of Civil, Mechanical and Environmental Engineering, The George Washington University

NATIONAL CENTER FOR EARTHQUAKE ENGINEERING RESEARCH
State University of New York at Buffalo
Red Jacket Quadrangle, Buffalo, NY 14261

PREFACE

The National Center for Earthquake Engineering Research (NCEER) is devoted to the expansion of knowledge about earthquakes, the improvement of earthquake-resistant design, and the implementation of seismic hazard mitigation procedures to minimize loss of lives and property. Initially, the emphasis is on structures and lifelines of the types that would be found in zones of moderate seismicity, such as the eastern and central United States.

NCEER's research is being carried out in an integrated and coordinated manner following a structured program. The current research program comprises four main areas:

- Existing and New Structures
- Secondary and Protective Systems
- Lifeline Systems
- Disaster Research and Planning

This technical report pertains to the second program area and, more specifically, to secondary systems.

In earthquake engineering research, an area of increasing concern is the performance of secondary systems which are anchored or attached to primary structural systems. Many secondary systems perform vital functions whose failure during an earthquake could be just as catastrophic as that of the primary structure itself. The research goals in this area are to:

1. Develop greater understanding of the dynamic behavior of secondary systems in a seismic environment while realistically accounting for inherent dynamic complexities that exist in the underlying primary-secondary structural systems. These complexities include the problem of tuning, complex attachment configuration, nonproportional damping, parametric uncertainties, large number of degrees of freedom and nonlinearities in the primary structure.
2. Develop practical criteria and procedures for the analysis and design of secondary systems.
3. Investigate methods of mitigation of potential seismic damage to secondary systems through optimization or protection. The most direct route is to consider enhancing their performance through optimization in their dynamic characteristics, in their placement within a primary structure or in innovative design of their supports. From the point of view of protection, base isolation of the primary structure or the application of other passive or active protection devices can also be fruitful.

Current research in secondary systems involves activities in all three of these areas. Their interaction and interrelationships with other NCEER programs are illustrated in the accompanying figure.

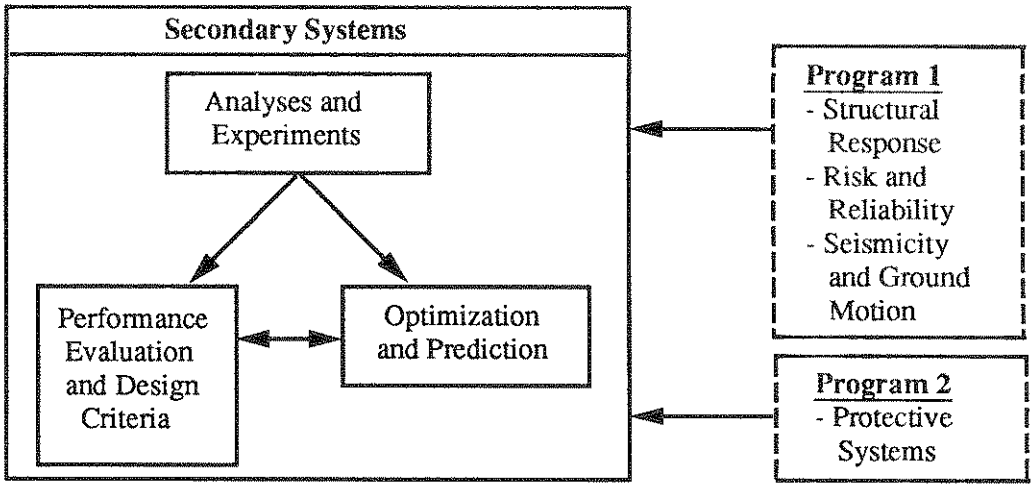

The purpose of research documented in this report is to develop a response spectrum approach for nonclassically damped structural systems. The aim is to make the procedure simple for practical applications and similar to the response spectrum procedure commonly used for analysis of classically damped systems. Emphasis is placed on nonclassically damped primary-secondary systems in which the effect of nonclassical damping is significant.

ABSTRACT

A response spectrum approach for analysis of nonclassically damped structural systems is presented. Similar to the response spectrum procedure for analysis of classically damped systems, the only required information regarding the ground motion input is its response spectrum. The procedure takes into account the effect of cross correlation between modes with closely spaced frequencies, and it is simple for practical application.

The proposed method is used to approximated the maximum response of several nonclassically damped structural systems. Emphasis is placed on nonclassically damped primary-secondary systems in which the effect of nonclassical damping is significant. Numerical results indicate that the maximum structural responses predicted by the proposed response spectrum approach are generally closer to the exact solutions than those obtained using approximate classically damped procedure. The accuracy of the present approach is quite reasonable.

ACKNOWLEDGEMENT

This work is supported by the National Center for Earthquake Engineering research, State University of New York at Buffalo under grant NCEER-87-2004.

TABLE OF CONTENTS

LIST OF ILLUSTRATIONS

LIST OF TABLES

SECTION 1

INTRODUCTION

In seismic analysis of multi-degree-of-freedom linear structures, modal analysis in conjunction with the response spectrum continues to be the most widely used technique, referred to as the response spectrum approach. The main reasons are the simplicity of the procedure and the fact that in most design situations the input ground acceleration is specified in terms of the displacement response spectrum (commonly referred to as the response spectrum).

Traditionally, the response spectrum approach requires the decoupling of the equations of motion using the undamped modes of vibration of the system. Then, the maximum response in each mode can be obtained using the response spectrum of the ground acceleration [2]. Then, the maximum value of the response quantities are determined using a proper modal combination rule [13]. Consequently, such as approach requires that the damping matrix of the structure is of the classical (proportional) form (i.e., the form specified by Caughey and O'Kelly [1]). However, real structural systems may not always be classically damped, so that the damping matrix may not be diagonalized by the eigenvectors of the undamped system. For these structures, referred to as nonclassically damped structures, the classical modal analysis is not applicable and the complex modal analysis procedure has been used in the literatures.

Response spectrum approaches for nonclassically damped structures have been suggested, recently, in the literature [9,12,6,11]. Based on the complex modal analysis, the maximum response of a nonclassically damped structure had been expressed in terms of the displacement response spectrum and the velocity response spectrum of the ground acceleration [6,11]. The velocity response

spectrum was obtained from the displacement response spectrum using various approximations [6,5].

In this paper an alternate approach is presented in which the equations of motion for a nonclassically damped structure are decoupled using the canonical modal decomposition approach [14]. The decoupled equations involve only real parameters and the maximum response of the structure is expressed in terms of the sine spectrum, that is related to the displacement response spectrum, as well as the cosine spectrum. The cosine spectrum is determined in approximation from the sine spectrum. A proper modal combination rule for sine and cosine spectra is derived and the maximum response quantities are determined taking into account the effect of cross correlation of modes with closely spaced frequencies. Similar to the response spectrum approach for analysis of classically damped structures, the present approach is simple for practical applications and only the information of the response spectrum for the ground acceleration input is needed.

The proposed response spectrum approach is employed to approximate the maximum response of a number of nonclassically damped primary-secondary structural systems. Particular emphasis is placed on evaluating the maximum response of primary-secondary structures in which the effect of nonclassical damping is known to be significant [14], including the tuning of the secondary system. Numerical results indicate that the accuracy of the proposed response spectrum approach is quite reasonable in comparison with the exact solution.

SECTION 2

BACKGROUND

The response of a linear n degree-of-freedom viscously damped structure subjected to a ground acceleration $\ddot{x}_g$, can be obtained by solving the following matrix equation of motion

$$\underline{M}\,\ddot{\underline{X}} + \underline{C}\,\dot{\underline{X}} + \underline{K}\,\underline{X} = -\,\underline{M}\,\underline{r}\,\ddot{x}_g \tag{1}$$

in which $\underline{M}$, $\underline{C}$, and $\underline{K}$ denote the (nxn) mass, damping, and stiffness matrices of the structure, respectively, and $\underline{X}$ is an n displacement vector relative to the moving base. The vector $\underline{r}$ is a unit vector $\underline{r} = [1, 1, \ldots, 1]'$. The super dot indicates differentiation with respect to time and an underbar denotes a vector or matrix. In Eq. (1), the argument of time, t, for $\underline{X}$ and $\ddot{x}_g$ has been omitted for simplicity.

Caughey and O'Kelly [1] showed that if the damping matrix satisfies the identity $\underline{C}\,\underline{M}^{-1}\,\underline{K} = \underline{K}\,\underline{M}^{-1}\,\underline{C}$, the matrix of the eigenvectors of the undamped system, $\underline{\Phi}$, can be used to transform the equations of motion into a set of n decoupled equations. The eigenvectors are found from the solution of the following

$$\omega_j^{\,2}\,\underline{M}\,\underline{\Phi}_j - \underline{K}\,\underline{\Phi}_j = 0 \tag{2}$$

in which $\omega_j^{\,2}$ and $\underline{\Phi}_j$ are the jth eigenvalue and eigenvector, respectively, where ω_j is the jth undamped natural frequency of the structure.

The equations of motion are decoupled using the transformation $\underline{X} = \underline{\Phi}\,\underline{Y}$ in Eq. (1), where $\underline{\Phi} = [\,\underline{\Phi}_1, \underline{\Phi}_2, \ldots, \underline{\Phi}_j]$ is the modal matrix. The jth decoupled equation of motion is given by [2]

$$\ddot{Y}_j + 2\xi_j\omega_j\,\dot{Y}_j + \omega_j^2\,Y_j = \psi_j\,\ddot{x}_g; \quad j = 1,2,\ldots,n \tag{3}$$

in which Y_j is the jth element of $\underline{Y}$, $\psi_j = -\underline{\Phi}_j'\,\underline{M}\,\underline{r} \,/\, \underline{\Phi}_j'\,\underline{M}\,\underline{\Phi}_j$ is the jth modal

participation factor, and $\xi_j = \underline{\Phi}_j' \underline{C} \underline{\Phi}_j / 2\omega_j$ is the jth modal damping ratio. In the expressions above, a prime denotes the transpose of a matrix or vector.

The solution of Eq. (3) can be expressed in terms of the well known Duhamel's integral

$$Y_j(t) = \psi_j \, h_j(t) \tag{4}$$

in which

$$h_j(t) = \frac{1}{\omega_{Dj}} \int_0^t \exp\left[-\xi_j \omega_j (t-\tau) \right] \sin \omega_{Dj}(t-\tau) \, \ddot{x}_g(\tau) \, d\tau \tag{5}$$

is the relative displacement with respect to the ground for a SDOF oscillator with frequency ω_j and damping ratio ξ_j. Note that $\omega_{Dj} = \omega_j (1 - \xi_j^2)^{1/2}$ is the jth damped frequency. Generally, the quantity of most interest is the maximum value of $Y_j(t)$, denoted by $\tilde{Y}_j$. For small values of damping (e.g., $\xi < 20\%$) it can be approximated by

$$\tilde{Y}_j = \psi_j \, S_v(\xi_j, \omega_j) / \omega_j \tag{6}$$

in which

$$S_v(\xi, \omega) = \left| \int_0^t \exp\left[-\xi\omega(t-\tau) \right] \sin \omega(t-\tau) \, \ddot{x}_g(\tau) d\tau \right|_{max} \tag{7}$$

is called the spectral pseudo-velocity response of the ground motion. Finally, the maximum value of the response vector $\underline{X}(t)$, denoted by $\tilde{\underline{X}}$, can be approximated by the well known square-root-of-sum-of-squares (SRSS) procedure

$$\tilde{\underline{X}} = \left[\sum_{j=1}^{n} \left[\underline{\Phi}_j \, \psi_j \, S_v(\xi_j, \omega_j)/\omega_j \right]^2 \right]^{1/2} \tag{8}$$

However, if the damping matrix, $\underline{C}$, is not of the classical form, the eigenvectors of the undamped system will not diagonalize the damping matrix. For such systems, the approach proposed by Foss [4] and Traill-Nash [10] can be used. In this approach, Eq. (1) is converted into a 2n first order matrix

equation

$$\underline{A}_1 \dot{\underline{Z}} + \underline{B}\,\underline{Z} = \underline{P}\,\ddot{x}_g \tag{9}$$

where $\underline{Z}$ is a 2n state vector, $\underline{Z} = \begin{Bmatrix} \dot{\underline{X}} \\ \cdots \\ \underline{X} \end{Bmatrix}$ and

$$A_1 = \left[\begin{array}{c|c} \underline{0} & \underline{M} \\ \hline \underline{M} & \underline{C} \end{array}\right], \quad B = \left[\begin{array}{c|c} -\underline{M} & \underline{0} \\ \hline \underline{0} & \underline{K} \end{array}\right], \quad \underline{P} = \begin{Bmatrix} \underline{0} \\ \cdots\cdots \\ -\underline{M}\,\underline{r} \end{Bmatrix} \tag{10}$$

The eigenvalue problem of Eq. (9), $|\lambda\,\underline{A}_1 + \underline{B}| = 0$, can be expressed as follows

$$\lambda_j\,\underline{A}_1\,\underline{\phi}_j + \underline{B}\,\underline{\phi}_j = 0 \tag{11}$$

in which λ_j and $\underline{\phi}_j$ are the jth eigenvalue and eigenvector, respectively. If the system is underdamped, the eigenvalues and eigenvectors are n pairs of complex conjugate. The jth pair of eigenvalues can be written as

$$\lambda_{2j-1,\,2j} = \xi_j\omega_j \pm i\,\omega_j\sqrt{1-\xi_j^2} = -\xi_j\omega_j \pm i\,\omega_{Dj} \tag{12}$$

in which $i = \sqrt{-1}$, $\omega_{Dj} = \omega_j(1-\xi_j^2)^{1/2}$, where ω_j is different from the jth natural frequency of the corresponding undamped system.

The response state vector, $\underline{Z}$, can be expressed as a linear combination of the eigenvectors

$$\underline{Z} = \underline{\phi}\,\underline{V} \tag{13}$$

where $\underline{\phi} = [\,\underline{\phi}_1,\ \underline{\phi}_2, \ldots,\ \underline{\phi}_n\,]$ is a (2nx2n) complex modal matrix. Substituting Eq. (13) into Eq. (9) and premultiplying it by the inverse of the $\underline{\phi}$ matrix, $\underline{\phi}^{-1}$, one obtains a set of 2n decoupled equations

$$\dot{V}_j = \lambda_j\,V_j + Q_j\,\ddot{x}_g \qquad ;\quad j = 1,2,\ldots,\,2n \tag{14a}$$

in which V_j and Q_j are the jth element of the $\underline{V}$ and $\underline{Q}$ vectors, where

$$\underline{Q} = \underline{\phi}^{-1}\begin{Bmatrix} -\underline{r} \\ \cdots \\ \underline{0} \end{Bmatrix}. \tag{14b}$$

Solutions of Eq. (14a) together with the transformation of Eq. (13) yield

the response state vector $\underline{Z}(t)$ of the structural system. Since λ_j and $\underline{\phi}_j$ are complex parameters that occur in complex conjugate pairs, the final response quantities are all real.

Igusa and Der Kiureghian [6], and Veletsos and ventura [11] expressed the solution of $\underline{Z}$, Eq.(13), in terms of the Duhamel's integral and its derivative

$$\underline{Z} = \sum_{j=1}^{n} \left[\underline{\alpha}_j \, h_j(t) + \underline{\beta}_j \, \dot{h}_j(t) \right] \tag{15}$$

in which $\underline{\alpha}_j = -2 \, \mathrm{Re}\left[\underline{\phi}_j Q_j \lambda_j \right]$ and $\underline{\beta}_j = 2 \, \mathrm{Re}\left[\underline{\phi}_j Q_j \right]$. In Eq. (15), $h_j(t)$ is the relative displacement of a SDOF system with frequency ω_j and damping ratio ξ_j given by Eq. (5); whereas $\dot{h}_j(t)$ is the relative velocity with respect to the ground. For classically damped systems, $\beta_j = 0$, and as expected, the response can be expressed in terms of $h_j(t)$ alone.

In practical design applications, the designer is provided with the description of the ground motion in terms of a response spectrum. The response spectrum is the plot of the maximum pseudo-velocity, $S_v(\xi,\omega)$, defined by Eq. (6) as a function of frequency ω and damping ratio ξ. The response spectrum also contains information regarding maximum relative displacement, $S_d(\xi,\omega)$, and the maximum pseudo-acceleration, $S_a(\xi,\omega)$, since they are related as follows

$$S_d(\xi,\omega) = S_v(\xi,\omega)/\omega \tag{16a}$$

$$S_a(\xi,\omega) = \omega \, S_v(\xi,\omega) \tag{16b}$$

These three quantities, i.e., $S_d(\xi,\omega)$, $S_v(\xi,\omega)$ and $S_a(\xi,\omega)$ are plotted in a single chart against frequency in a so-called tripartite logarithmic plot.

It follows from Eq. (15) that the determination of the maximum response of a nonclassically damped structure requires not only the maximum relative displacement $S_d(\xi,\omega)$ but also the maximum relative velocity, $\tilde{\dot{h}}(\xi,\omega) = \text{maxi.} \, |\dot{h}(t)|$. Note that the maximum relative velocity, $\tilde{\dot{h}}(\xi,\omega)$, is different

from the maximum pseudo velocity, $S_v(\xi,\omega)$. Since, however, the maximum relative displacement $S_d(\xi,\omega)$ is the only information available to a designer, it is desirable to obtain the maximum velocity, $\dot{\tilde{h}}(\xi,\omega)$, in term of $S_d(\xi,\omega)$. Attempts in this regard have been made by several researchers in the following.

Villaverde and Newmark [12] assumed that for small values of damping ratio ξ, the maximum relative velocity, $\dot{\tilde{h}}(\xi,\omega)$, can be approximated by the maximum pseudo velocity $S_v(\xi,\omega)$. When the ground acceleration excitation is assumed to be a stationary white noice process, the relation between the maximum relative velocity $\dot{\tilde{h}}(\xi,\omega)$ and the maximum relative displacement $S_d(\xi,\omega)$ can be obtained in approximation. Such a relationship was assumed to hold for general earthquake excitations to obtain $\dot{\tilde{h}}(\xi,\omega)$ from $S_d(\xi,\omega)$ by Igusa and Der Kiureghian [6].

Gupta and Jaw [5] compared the maximum relative velocity, $\dot{\tilde{h}}(\xi, \omega)$, and the maximum relative displacement, $S_d(\xi,\omega)$, for several earthquake records in different frequency ranges and concluded that for intermediate values of ω (i.e., $1< \omega <10$ hz.), the maximum realtive velocity $\dot{\tilde{h}}(\xi,\omega)$ can be approximated by the maximum pseudo-velocity $S_v(\xi,\omega)$. Further, procedures are proposed for approximating the maximum relative velocity $\dot{\tilde{h}}(\xi,\omega)$ using the knowledge of the maximum relative displacement $S_d(\xi,\omega)$ for other frequency ranges.

In this paper, we propose an alternate approach for approximating the maximum response of a nonclassically damped system from the knowledge of the response spectrum, $S_d(\xi,\omega)$. This is accomplished using the "canonical modal analysis" formulated by the authors for the analysis of nonclassically damped structures [14].

SECTION 3

CANONICAL MODAL ANALYSIS

The equations of motion for the state vector, Eq. (9), are rewritten as follows:

$$\dot{\underline{Z}} = \underline{A}\,\underline{Z} + \underline{W}\,\ddot{x}_g \tag{17}$$

where

$$\underline{A} = \left[\begin{array}{c|c} \underline{M}^{-1}\underline{C} & -\underline{M}^{-1}\underline{K} \\ \hline \underline{I} & \underline{0} \end{array}\right] \quad ; \quad \underline{W} = \left\{\begin{array}{c} -\underline{r} \\ \cdots \\ \underline{0} \end{array}\right\} \tag{18}$$

The eigenvalues and eigenvectors of matrix $\underline{A}$ are identical to those of Eq. (11), denoted by λ_j and $\underline{\phi}_j$, respectively, for $j = 1, 2, \ldots, 2n$, see Eq. (12). Further, the jth pair of eigenvectors can be expressed as

$$\underline{\phi}_{2j-1} = \underline{a}_j + i\,\underline{b}_j \tag{19}$$

$$\underline{\phi}_{2j} = \underline{a}_j - i\,\underline{b}_j \quad , \qquad j = 1, 2, \ldots, n$$

in which $\underline{a}_j$ and $\underline{b}_j$ are 2n real vectors

The (2nx2n) real matrix $\underline{T}$ constructed in the following

$$\underline{T} = \left[\underline{a}_1, \underline{b}_1, \underline{a}_2, \underline{b}_2, \ldots, \underline{a}_j, \underline{b}_j, \ldots, \underline{a}_n, \underline{b}_n\right] \tag{20}$$

will transform the matrix $\underline{A}$ into a canonical form $\underline{\Lambda}$, i.e.,

$$\underline{\Lambda} = \underline{T}^{-1}\,\underline{A}\,\underline{T} \tag{21}$$

in which $\underline{T}^{-1}$ is the inverse of the $\underline{T}$ matrix and

$$\underline{\Lambda} = \begin{bmatrix} \underline{\Lambda}_1 & & & 0 \\ & \underline{\Lambda}_2 & & \\ & & \ddots & \\ 0 & & & \underline{\Lambda}_n \end{bmatrix} \tag{22}$$

where

$$\underline{\Lambda}_j = \begin{bmatrix} -\xi_j\omega_j & \omega_{Dj} \\ -\omega_{Dj} & -\xi_j\omega_j \end{bmatrix} \qquad , \; j = 1, 2, \ldots, n \tag{23}$$

Let the transformation of the state vector be

$$\underline{Z} = \underline{T}\ \underline{\nu} \tag{24}$$

Substituting Eq. (24) into Eq. (17) and premultiplying it by the inverse of the $\underline{T}$ matrix, $\underline{T}^{-1}$, one obtains

$$\dot{\underline{\nu}} = \underline{\Lambda}\ \underline{\nu} + \underline{F}\ \ddot{x}_g \tag{25}$$

in which $\underline{\Lambda}$ is given by Eqs. (22) and (23), and

$$\underline{F} = \underline{T}^{-1} \begin{Bmatrix} -\underline{r} \\ \cdots \\ \underline{0} \end{Bmatrix} \tag{26}$$

Equation (25) consists of n pairs of decoupled equations. Each pair of equations represents one vibrational mode, and it is uncoupled with other pairs. However, the two equations in each pair are coupled. The transformation given in Eq. (24) is referred to as the canonical transformation [14]. All the parameters in Eq. (25) are real.

The jth pair of coupled equations in Eq. (25), corresponding to the jth vibrational mode, is given as follows:

$$\dot{\nu}_{2j-1} = -\xi_j \omega_j\ \nu_{2j-1} + \omega_{Dj}\ \nu_{2j} + F_{2j-1}\ \ddot{x}_g \tag{27a}$$

$$\dot{\nu}_{2j} = -\omega_{Dj}\ \nu_{2j-1} - \xi_j \omega_j\ \nu_{2j} + F_{2j}\ \ddot{x}_g \tag{27b}$$

in which F_{2j-1} and F_{2j} are the 2j-1th and the 2jth elements of the $\underline{F}$ vector, respectively. Solutions of Eqs. (27) together with the transformation of Eq. (24) yield the response state vector $\underline{Z}(t)$ of the structural system.

The advantage of the formulation given above is that the computations for the solutions are all in the real field. The modal decomposition approach described above is referred to as the canonical modal decomposition.

There are a number of procedures that can be used to solve Eqs. (27) as explained in details in Ref. 14. Let $\underline{h}_{\nu_j}(t)$ be the impulse response function of the jth vibrational mode, i.e., $\ddot{x}_g = \delta(t)$ and $\underline{\nu}_j(t) = [\nu_{2j-1}, \nu_{2j}]' = \underline{h}_{\nu_j}(t)$

where $\delta(t)$ is the Dirac delta function. Then $\underline{h}_{\nu_j}(t)$ can be easily obtained from Eq. (27) as

$$\underline{h}_{\nu_j}(t) = \begin{Bmatrix} (e^{-\xi_j\omega_j t} \cos \omega_{Dj} t)\ F_{2j-1} + (e^{-\xi_j\omega_j t} \sin \omega_{Dj} t)\ F_{2j} \\ -(e^{-\xi_j\omega_j t} \sin \omega_{Dj} t)\ F_{2j-1} + (e^{-\xi_j\omega_j t} \cos \omega_{Dj} t)\ F_{2j} \end{Bmatrix} \tag{28}$$

The response of the jth vibrational mode $\underline{\nu}_j(t) = [\nu_{2j-1},\ \nu_{2j}]'$ is given by

$$\underline{\nu}_j(t) = \int_0^t \underline{h}_{\nu_j}(t-\tau)\ \ddot{x}_g(\tau)\ d\tau \qquad j = 1,\ 2,\ \ldots n \tag{29}$$

Using Eq. (29) and the transformation of Eq. (24), the displacement vector can be expressed as:

$$\underline{X}(t) = \sum_{j=1}^{n} \left[\ \underline{\Gamma}_j\ S_j(t) + \underline{\Delta}_j\ C_j(t)\right] \tag{30}$$

in which

$$\underline{\Gamma}_j = \underline{a}_{jL}\ F_{2j} - \underline{b}_{jL}\ F_{2j-1} \tag{31a}$$

$$\underline{\Delta}_j = \underline{a}_{jL}\ F_{2j-1} + \underline{b}_{jL}\ F_{2j} \tag{31b}$$

$$S_j(t) = \int_0^t e^{-\xi_j\omega_j(t-\tau)} \sin \omega_{Dj}(t-\tau)\ \ddot{x}_g(\tau)\ d\tau \tag{31c}$$

$$C_j(t) = \int_0^t e^{-\xi_j\omega_j(t-\tau)} \cos \omega_{Dj}(t-\tau)\ \ddot{x}_g(\tau)\ d\tau \tag{31d}$$

where $\underline{a}_{jL}$ and $\underline{b}_{jL}$ are the lower halves of the $\underline{a}_j$ and $\underline{b}_j$ vectors, respectively.

For classically damped structures, the vector $\underline{\Delta}_j$ can be shown to be null and, as expected, the response reduces to terms involving the sine integrals $S_j(t)$ only. Of course, the maximum value of integrals involving the sine terms is nothing but the pseudo-velocity $S_v(\xi,\omega)$ which can be obtained from

the response spectrum $S_d(\xi,\omega)$, Eq. (16a).

For nonclassically damped systems, the maximum response involves not only sine integrals, $S_j(t)$, but also cosine integrals, $C_j(t)$. The following section outlines a simple procedure that can be used to evaluate the maximum of cosine integrals from the pseudo-velocity spectrum of the ground motion, i.e., maximum of the sine integrals.

SECTION 4

EVALUATION OF COSINE SPECTRUM

The maximum value of $S_j(t)$ that involves sine integral denoted by $\tilde{S}_j$ = maxi. $|S_j(t)|$, is nothing but the pseudo-velocity, i.e., $\tilde{S}_j = S_v(\xi_j,\omega_j) = \omega_j S_d(\xi_j,\omega_j)$. The plot of $\tilde{S}_j$ against the frequency, ω_j, for a given damping ratio, ξ_j, is the pseudo-velocity spectrum, and herein referred to as the "sine spectrum". The maximum value of $C_j(t)$ that involves cosine integral Eq. (31), is denoted by $\tilde{C}_j$ = maxi. $|C_j(t)|$. The plot of $\tilde{C}_j$ against the frequency, ω_j, for a given damping ratio, ξ_j, is herein referred to as the "cosine spectrum". Note that $\tilde{S}_j$ and $\tilde{C}_j$ (or sine and cosine spectra) are functions of ω_j and ξ_j, and because of simplicity in notation these arguments are omitted.

The pseudo-velocity spectrum of an earthquake record can be generated either directly by numerical integration of Eq. (5) or using an approximate procedure developed by Newmark, Blume and Kapur [8]. In the latter case the pseudo-velocity spectrum (or the sine spectrum) is approximated by the knowledge of the maximum values of the ground acceleration, ground velocity and ground displacement. Such an approximate procedure is based on an empirical study of the response spectra of a large number of earthquake records.

In this study, the pseudo-velocity spectrum or the sine spectrum will be obtained using either one of the two approaches mentioned above, whereas the cosine spectrum will be evaluated, in approximation, from the sine spectrum.

In order to evaluate the approximate relation between the sine spectrum and the cosine spectrum, the earthquake ground acceleration $\ddot{x}_g(t)$ is modeled expediently as a uniformly modulated nonstationary random process with zero mean

$$\ddot{x}_g(t) = \alpha(t)\ \ddot{x}_0(t) \tag{32}$$

in which $\alpha(t)$ is a deterministic non-negative modulating or envelope function and $\ddot{x}_0(t)$ is a stationary random process with zero mean and a power spectral density, $\phi_{\ddot{x}\ddot{x}}(\omega)$. The stationary random process $\ddot{x}_0(t)$ can be expressed in terms of a summation of sine functions as follows

$$\ddot{x}_0(t) = \sum_{k=1}^{N} A_k \sin(\omega_k t + \phi_k) \tag{33a}$$

in which ϕ_k's are independent random phase angles distributed uniformly in $[0,2\pi]$ and $A_k = \left[2\phi_{\ddot{x}\ddot{x}}(\omega_k)\ \Delta\omega \right]^{1/2}$ with $\phi_{\ddot{x}\ddot{x}}(\omega_k)$ being the power spectral density of $\ddot{x}_0(t)$ evaluated at frequency $\omega_k = k\Delta\omega$. A commonly used form of the spectral density, $\phi_{\ddot{x}\ddot{x}}(\omega)$, is that given by [2,7]

$$\phi_{\ddot{x}\ddot{x}}(\omega) = \frac{1+4\xi_g^2(\omega/\omega_g)^2}{\left[1-(\omega/\omega_g)^2\right]^2 + 4\xi_g^2(\omega/\omega_g)^2} * \frac{(\omega/\omega_0)^4}{\left[1-(\omega/\omega_0)^2\right]^2 + 4\xi_0^2(\omega/\omega_0)^2} S^2 \tag{33b}$$

in which ξ_g, ω_g, ξ_0, ω_0, and S are parameters depending on the intensity and the characteristics of the earthquake at a particular geological location.

Various types of the envelope function $\alpha(t)$ have been suggested in the literature to introduce the nonstationarity of the ground acceleration into Eq. (32). One possible form of $\alpha(t)$ is: $\alpha(t) = (t/t_1)^2$ for $0 \le t \le t_1$, $\alpha(t) = 1$ for $t_1 \le t \le t_2$, and $\alpha(t) = \exp\left[\beta(t-t_2)\right]$ for $t > t_2$. Note that t_1, t_2 and β can be selected to reflect the shape and duration of the earthquake ground acceleration. When $\alpha(t) = 1$, the ground acceleration is a stationary random process. The stationary assumption is reasonable when the duration of the strong shaking of the earthquake ground motion is much longer than the natural period of the structure.

Thus, the earthquake ground acceleration can be expressed as follows

$$\ddot{x}_g(t) = \sum_{k=1}^{N} \alpha(t)\ A_k \sin(\omega_k t + \phi_k) \tag{34}$$

Note that for a given set of ϕ_k values (k=1, 2,..., N), Eq. (34) represents a sample time history of the ground acceleration $\ddot{x}_g(t)$. Substituting Eq. (34) into Eq. (31) and changing $t-\tau$ to a new integration variable τ, one obtains

$$S_j(t) = \sum_{k=1}^{N} \int_0^t \alpha(t-\tau)\, A_k \sin\left[\omega_k(t-\tau) + \phi_k\right] e^{-\xi_j \omega_j \tau} \sin \omega_{Dj}\tau \, d\tau \qquad (35a)$$

$$C_j(t) = \sum_{k=1}^{N} \int_0^t \alpha(t-\tau)\, A_k \sin\left[\omega_k(t-\tau) + \phi_k\right] e^{-\xi_j \omega_j \tau} \cos \omega_{Dj}\tau \, d\tau \qquad (35b)$$

It is mentioned that ω_k's for k = 1,2..., N are the frequency values of the power spectral density of the random process $\ddot{x}_0(t)$; whereas ω_j and ξ_j are the natural frequency and damping ratio of the single-degree-of-freedom oscillator.

The maximum values of expressions in Eqs. (35a) and (35b) have been denoted by $\tilde{S}_j$ and $\tilde{C}_j$, respectively. $\tilde{C}_j$ will be obtained in approximation as follows.

When ω_j is very small, both the exponential term, $e^{-\xi_j \omega_j \tau}$, and the cosine term, $\cos \omega_{Dj}\tau$, in Eq. (35b) can be approximated by unity. This results in

$$\begin{aligned} C_j(t) &= \sum_{k=1}^{N} \int_0^t A_k\, \alpha(t-\tau) \sin\left[\omega_k(t-\tau) + \phi_k\right] d\tau \\ &= \sum_{k=1}^{N} \int_0^t A_k\, \alpha(\tau) \sin(\omega_k\tau + \phi_k)\, d\tau = \int_0^t \ddot{x}_g(\tau)\, d\tau \qquad (36) \\ &= \dot{x}_g(t) \end{aligned}$$

Therefore, the maximum value of $C_j(t)$ for small ω_j is the maximum ground velocity, i.e., $\tilde{C}_j = \text{maxi.} \left|\dot{x}_g(t)\right|$. In other words, the cosine spectrum in the small frequency range is equal to the maximum earthquake ground velocity.

When ω_j is very large, the natural period T_j of the oscillator is very short and hence the stationary period of the earthquake is much longer than the oscillator period T_j. Thus, the maximum values $\tilde{C}_j$ and $\tilde{S}_j$ will occur in the stationary portion of the response. Consequently, the earthquake ground acceleration can be modeled as a stationary random process, i.e., $\alpha(t) = 1$, and $C_j(t)$ can be expressed as

$$C_j(t) = \sum_{k=1}^{N} \int_0^t A_k \sin[\omega_k(t-\tau) + \phi_k] \, e^{-\xi_j \omega_j \tau} \cos \omega_{Dj} \tau \, d\tau \tag{37}$$

Using exponential relations (Euler's equation) for the sine terms and cosine terms in Eq. (37), the integral can be evaluated as

$$\begin{aligned} C_j(t) = \sum_{k=1}^{N} \frac{A_k}{4} \Bigg\{ & \left[e^{\underline{i}(\omega_{Dj} t + \phi_k) - \xi_j \omega_j t} - e^{\underline{i}(\omega_k t + \phi_k)} \right] / (\omega_k - \omega_{Dj} - \underline{i}\xi_j \omega_j) \\ & + \left[e^{\underline{i}(-\omega_{Dj} t + \phi_k) - \xi_j \omega_j t} - e^{+\underline{i}(\omega_k t + \phi_k)} \right] / (\omega_k + \omega_{Dj} - \underline{i}\xi_j \omega_j) \\ & + \left[e^{\underline{i}(\omega_{Dj} t - \phi_k) - \xi_j \omega_j t} - e^{-\underline{i}(\omega_k t + \phi_k)} \right] / (\omega_k + \omega_{Dj} + \underline{i}\xi_j \omega_j) \\ & + \left[e^{-\underline{i}(\omega_{Dj} t + \phi_k) - \xi_j \omega_j t} - e^{-\underline{i}(\omega_k t + \phi_k)} \right] / (\omega_k - \omega_{Dj} + \underline{i}\xi_j \omega_j) \Bigg\} \end{aligned} \tag{38}$$

When ω_j is large compare to ω_k, the above expression can be approximated by

$$C_j(t) = \frac{1}{\omega_j^2} \left[\xi_j \omega_j \, \dot{x}_g(t) + \ddot{x}_g(t) \right] + \frac{1}{\omega_j^2} \, e^{-\xi_j \omega_j t} \sum_{k=1}^{N} A_k \, B_{kj}(t) \tag{39a}$$

in which

$$B_{kj}(t) = \omega_j \sin \omega_{Dj} t \sin\phi_k - \cos \omega_{Dj} t \, (\omega_k \cos \phi_k + \xi_j \omega_j \sin\phi_k) \tag{39b}$$

Let t^* be the time at which $C_j(t)$ reaches its maximum value, i.e., $\tilde{C}_j = C_j(t^*)$. Then, Eq. (39a) becomes

$$\tilde{C}_j = \frac{1}{\omega_j^2}\left[\xi_j\omega_j\,\ddot{x}_g(t^*) + \dot{\ddot{x}}_g(t^*)\right] + \frac{1}{\omega_j^2}\,e^{-\xi_j\omega_j t^*}\sum_{k=1}^{N} A_k\,B_{kj}(t^*) \qquad (40)$$

For $\xi_j \neq 0$, Eq. (40) can be further simplified to

$$\tilde{C}_j = \frac{1}{\omega_j^2}\left[\,\xi_j\omega_j\,\ddot{x}_g(t^*) + \dot{\ddot{x}}_g(t^*)\,\right] \qquad (41a)$$

since the summation of $\sin\phi_k$ or $\cos\phi_k$ for k=1,2,...,N is close to zero.

Eq. (41a) represents the maximum value of $C_j(t)$ when ω_j is large. Note that ξ_j is generally much smaller than unity. Examination of Eq. (41a) reveals that <u>when ω_j is not extremely large, $\tilde{C}_j$ can be approximated as being inversely proportional to ω_j^2</u>.

On the other hand, when ω_j is extremely large, $\xi_j\omega_j\,\ddot{x}_g(t)$ is the dominant term and $\tilde{C}_j$ reduces to

$$\tilde{C}_j = \xi_j\,\ddot{x}_g(t)/\omega_j \qquad (41b)$$

In a similar manner using Eq. (35a) with $\alpha(t) = 1$, the following approximate expression for the sine spectrum $S_j(t)$ for ω_j very large can be obtained as

$$S_j(t) = \ddot{x}_g(t)/\omega_j + e^{-\xi_j\omega_j t}\sum_{k=1}^{N} A_k(-\xi_j\omega_j\,\sin\omega_{Dj}t\,\cos\phi_k + \sin\omega_{Dj}t\,\sin\phi_k + \omega_{Dj}\,\sin\omega_{Dj}t\,\cos\phi_k) \qquad (42)$$

If $\hat{t}$ denotes the time at which $S_j(t)$ reaches its maximum value, i.e., $\tilde{S}_j = S_j(\hat{t})$, then Eq. (42) can be simplified as

$$\tilde{S}_j = \ddot{x}_g(\hat{t})/\omega_j = \text{maxi.}\left|\ddot{x}_g(t)/\omega_j\right| \qquad (43)$$

provide that $\xi_j \neq 0$. Equation (43) indicates that in the high frequency region (i.e., ω_j very large), the relative pseudo-spectral acceleration $\omega_j\,\tilde{S}_j$, is constant and equal to maximum ground acceleration $\ddot{x}_g(t)$ as expected.

A comparison of Eqs. (41b) and (43) indicates that when ω_j is extremely large and $\xi_j \neq 0$, the cosine spectrum is related to the sine spectrum as follows

$$\tilde{C}_j = \xi_j \tilde{S}_j \tag{44}$$

In the intermediate frequency range for ω_j, closed form expressions for $\tilde{S}_j$ and $\tilde{C}_j$ are not tractable. However, for a comparison of $\tilde{S}_j$ and $\tilde{C}_j$, the ground acceleration $\ddot{x}_g(t)$ is approximated by stationary white noise with zero mean and a power spectral density S_0. Then, $C_j(t)$ and $S_j(t)$ are stationary random process with zero mean and their mean square values (or variance) can be obtained as follows (see Appendix).

$$E\left[C_j^2(t)\right] = \left[(1 + \xi_j^2)/2\xi_j\omega_j\right] \pi S_0 \tag{45a}$$

$$E\left[S_j^2(t)\right] = \left[(1 - \xi_j^2)/2\xi_j\omega_j\right] \pi S_0 \tag{45b}$$

It follows from above equations that for small damping ξ_j the variances of $S_j(t)$ and $C_j(t)$ are identical. Thus, the maximum values of $C_j(t)$ and $S_j(t)$ are approximately equal, i.e., $\tilde{C}_j \approx \tilde{S}_j$. This, indeed, has been verified by comparing the exact $\tilde{C}_j$ and $\tilde{S}_j$ values for several earthquake records for intermediate values of ω_j.

Noted that in most situations the response spectrum used for design purposes is approximated by a series of straight lines in the tripartite logarithmic paper and it is referred to as a smooth spectrum herein. These straight lines correspond to regions of amplification of the ground acceleration, velocity and displacement. There are also guidelines available that can be used to approximate a smooth spectrum based on only the knowledge of the maximum ground acceleration, velocity and displacement [8]. Therefore the cosine spectrum will be obtained in approximation from the available smooth sine spectrum using the results derived above. This will lead to a smooth cosine spectrum, and the procedures are described in the following.

Exact sine and cosine spectra for several earthquakes have been constructed and all sine spectra have been smoothled out with straight lines.

A comparison between the smooth sine spectrum with the respective cosine spectrum indicates that at low frequency values of ω_j, the cosine spectrum is constant and is equal to maximum value of ground velocity, Eq. (36), up to the frequency value, ω_a, at which it intersects the sine spectrum as shown in Fig. 1 by segment 1. This point of intersection, ω_a, determines the beginning of the intermediate region in which the two spectra are almost identical. The upper frequency, ω_b, at which the two spectra are almost identical can be well approximated by the largest frequency at which the sine spectrum is equal to a constant amplification of the ground acceleration. This frequency, ω_b, can easily be determined from the smooth sine spectrum, see Fig. 1. Beyond ω_b, the cosine spectrum can be well approximated by a straight line on the log-log paper with a slope of -1, see Eq.(41a), as shown in Fig. 1 by the segment (3).

When ω_j is extremely large, the cosine spectrum can be approximated by multiplying the sine spectrum by the damping ratio ξ_j as shown in Eq.(44). Thus, in the extremely large frequency region, say $\omega_j > 100$ cps, a straight line parallel to the sine spectrum but its ordinate being equal to $\xi_j \tilde{S}_j$ can be drawn as shown in Fig. 1 by the segment (4). The intersection of segments (3) and (4), denoted by ω_c, is the beginning of the region where $\tilde{C}_j \approx \xi_j \tilde{S}_j$, Eq. (44).

Thus, the cosine spectrum is completely define if the maximum value of the ground velocity is known. Note that the values of the maximum ground acceleration and ground displacement can be obtained from the sine spectrum. Unfortunately, the value of the maximum ground velocity cannot be directly extracted from the sine spectrum. Based on empirical study of a large number of earthquakes, the average values for the maximum ground velocity was expressed in terms of the maximum ground acceleration and the site condition, (i.e., soil type), in Ref.8. For rock, the maximum values of ground velocity

and ground displacement are 36 in/sec. and 12 in., respectively, for every 1 g in/sec.^{2} of maximum ground acceleration. For alluvium, the maximum values of ground velocity and displacement are 48 in/sec. and 36 in, respectively, for every 1 g in/sec^2 of maximum ground acceleration. Therefore, by comparing the above values with the maximum values of ground acceleration and displacement obtained from the sine spectrum, one can determine the soil types and the approximate maximum value of the ground velocity.

Figures 2a through 2h presents the exact and smooth sine spectra for several earthquake ground accelerations. Also shown in these figures are the approximate smooth cosine spectrum obtained from the knowledge of the smooth sine spectrum. For comparison purposes the exact cosine spectrum which was obtained using a numerical itegration of Eq. 35b is also presented.

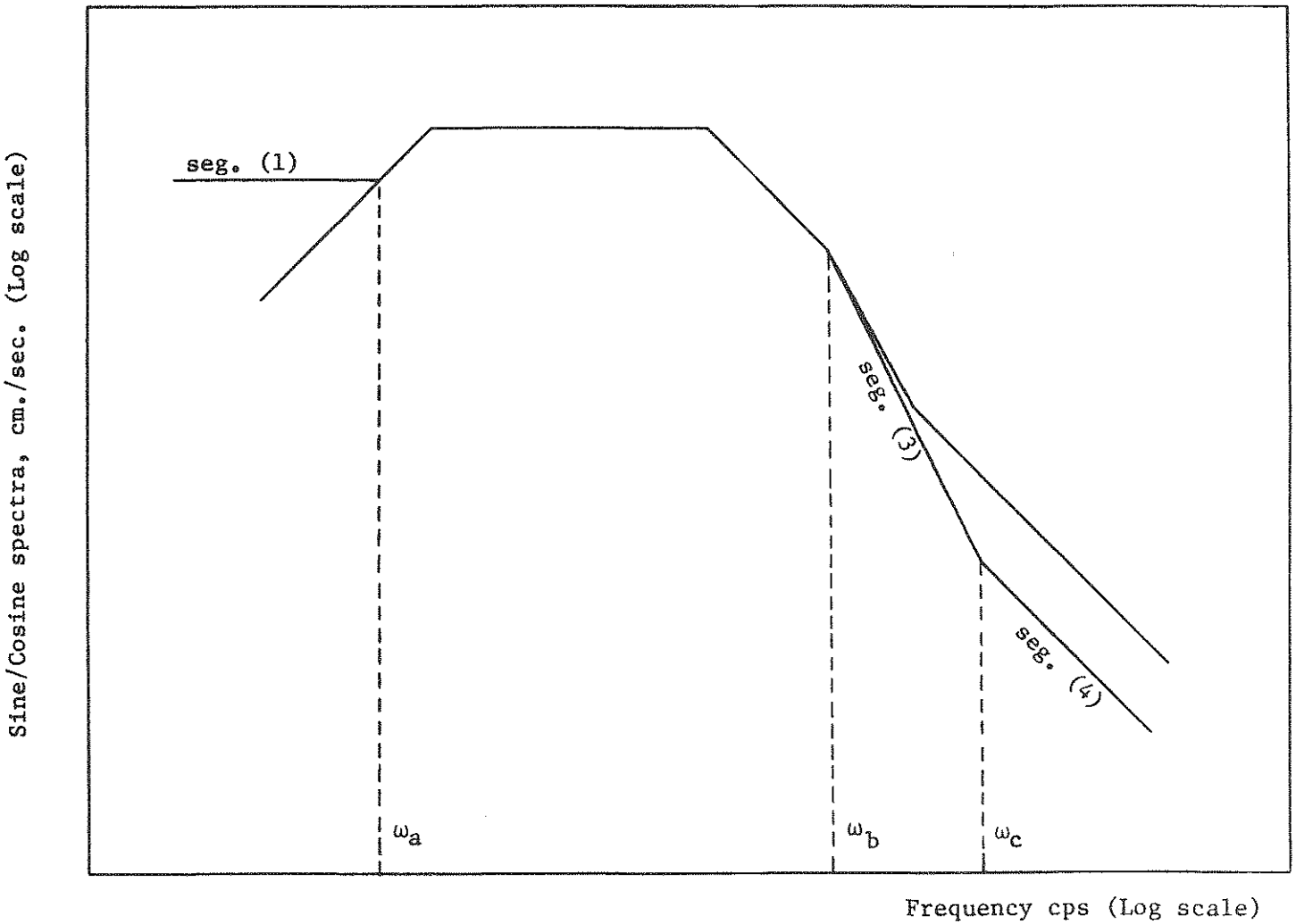

Fig. 1 Smooth Sine and Cosine Spectra

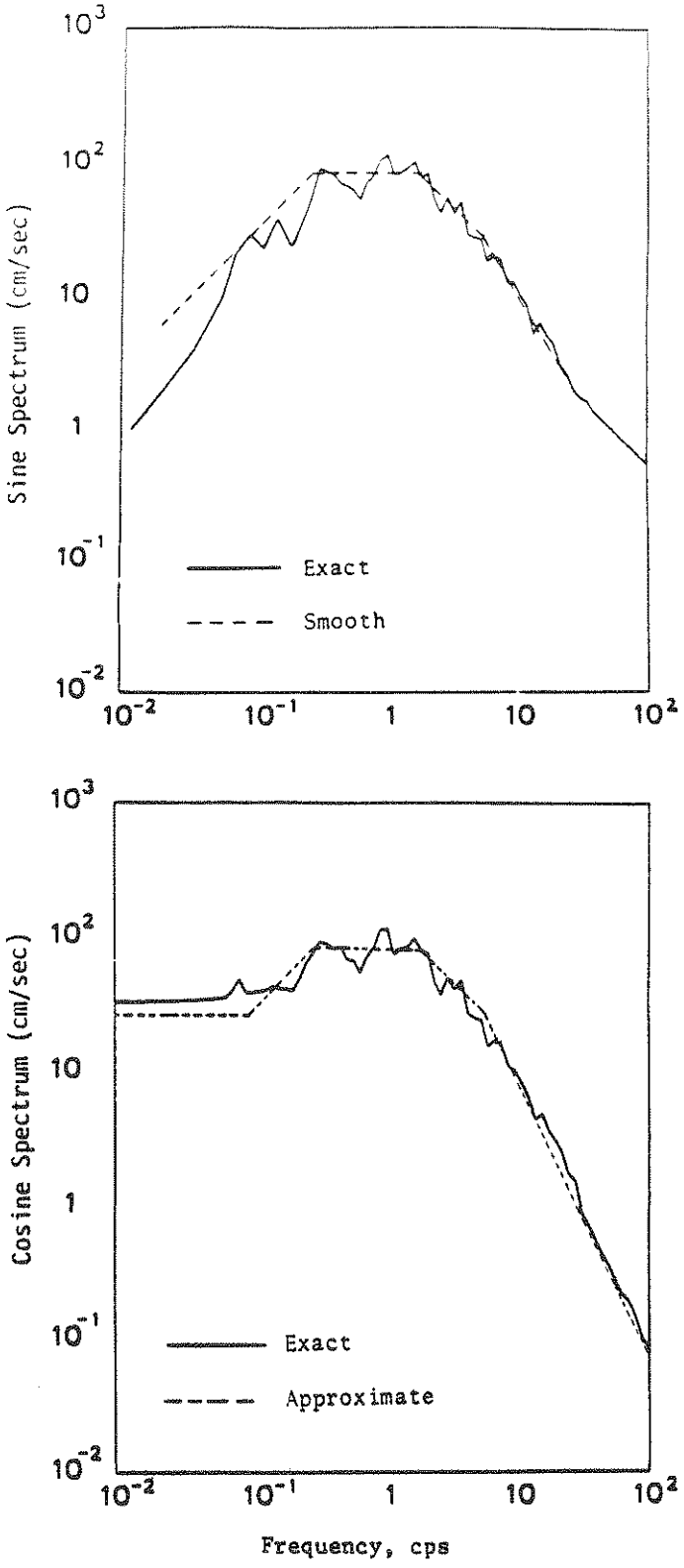

FIGURE 2a Sine and Cosine Spectra for El Centro Earthquake, ξ = 2%

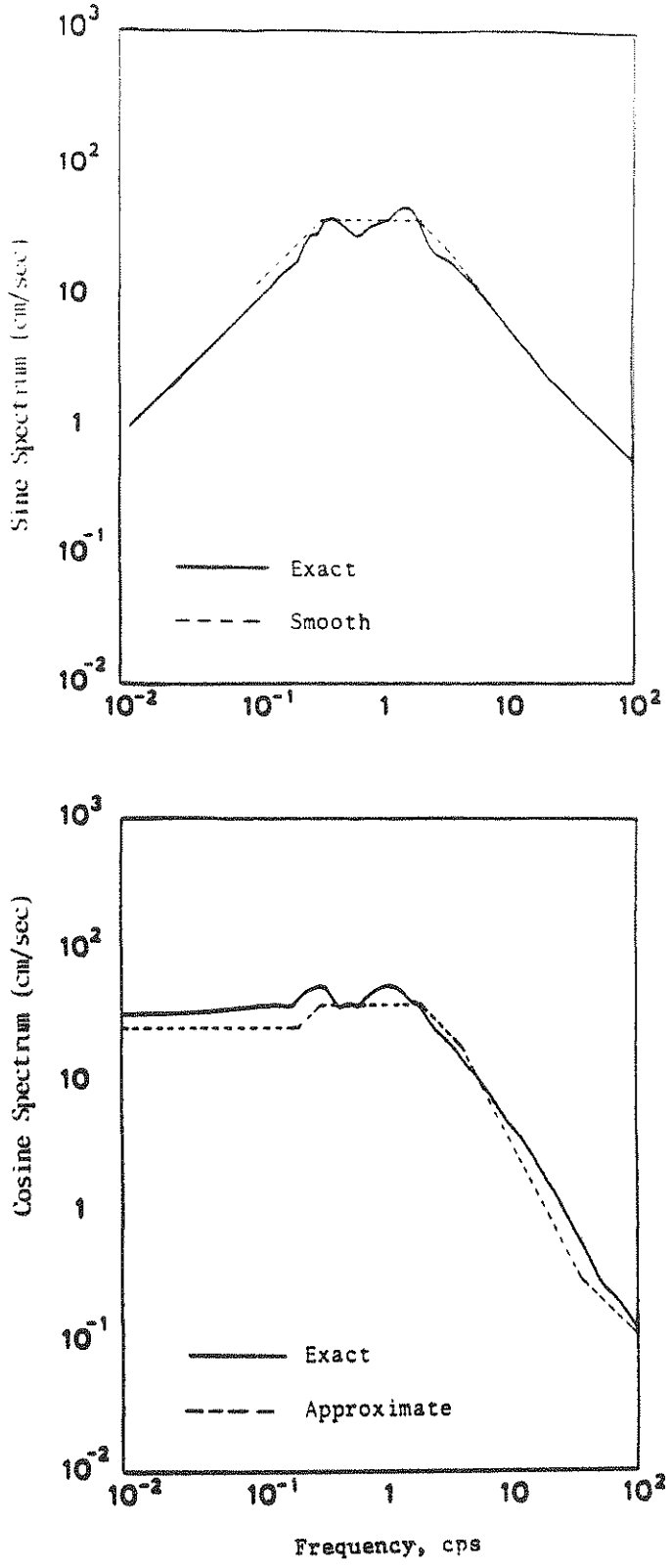

FIGURE 2b Sine and Cosine Spectra for El Centro Earthquake, ξ = 20%

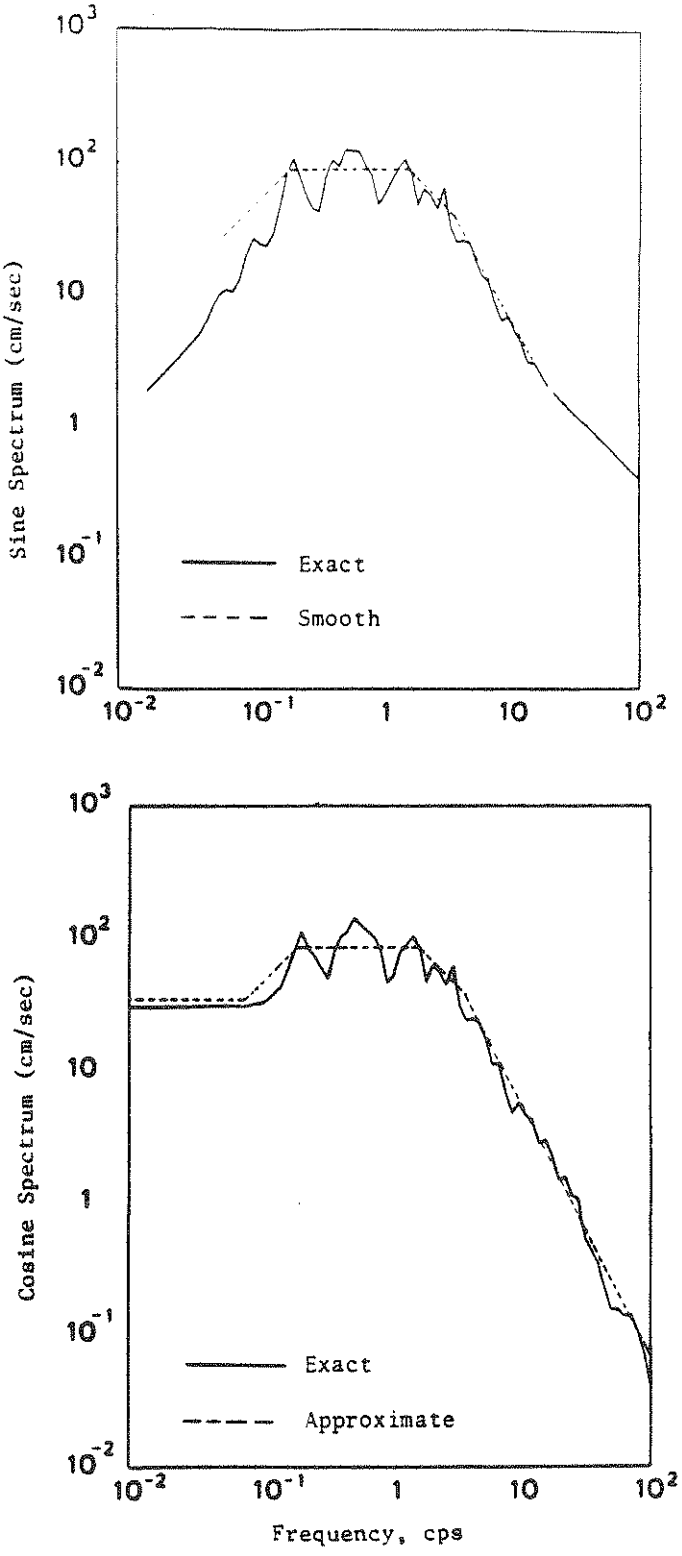

FIGURE 2c Sine and Cosine Spectra for San Fernando Earthquake ξ = 2%

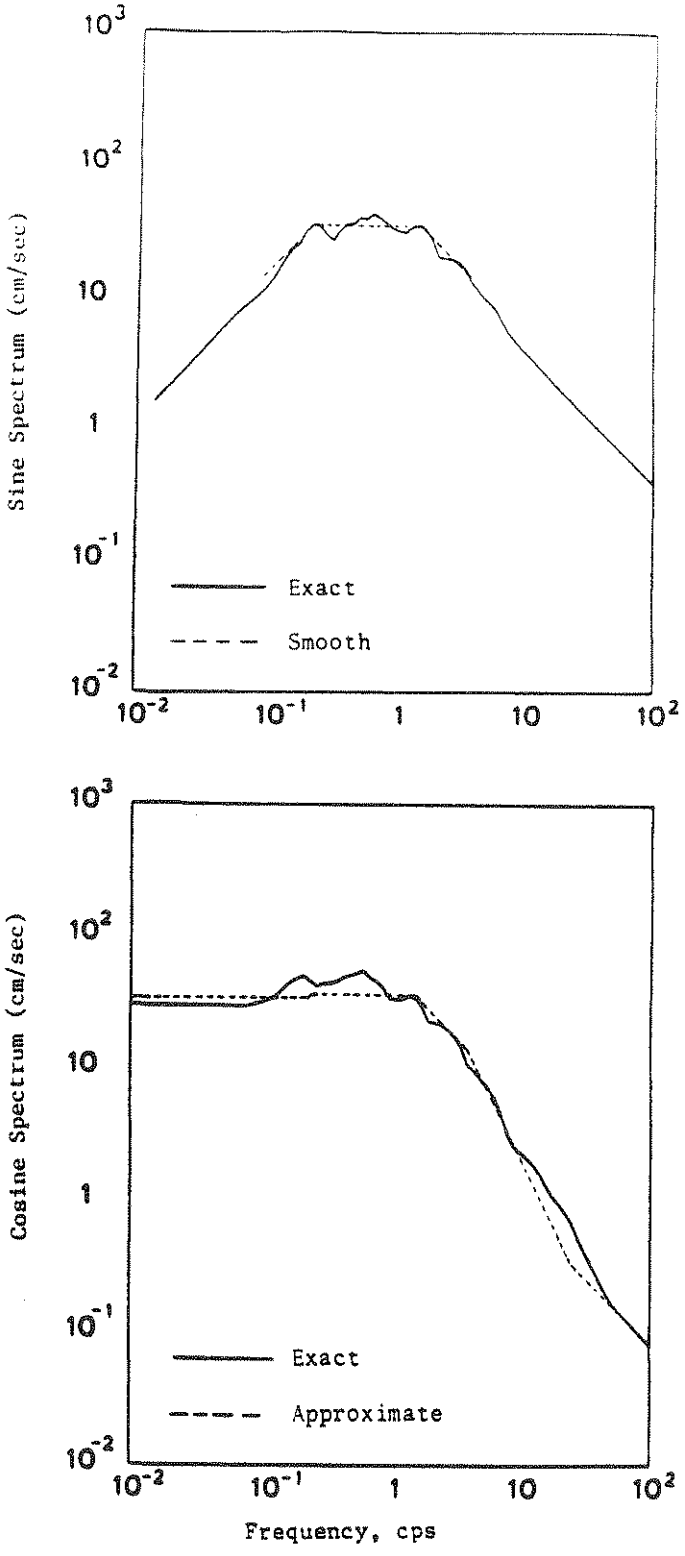

FIGURE 2d Sine and Cosine Spectra for San Fernando Earthquake, ξ = 20%

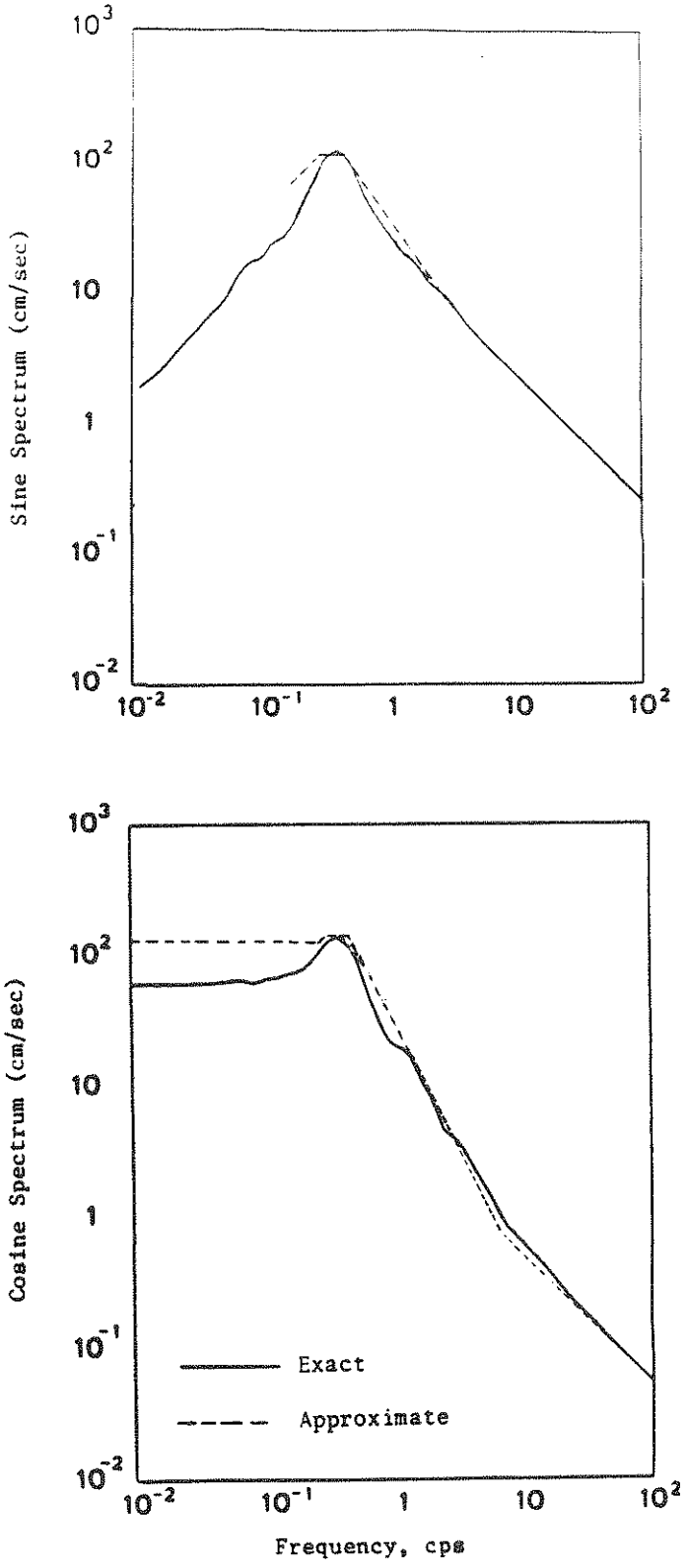

FIGURE 2e Sine and Cosine Spectra for Mexico City Earthquake, ξ = 2%

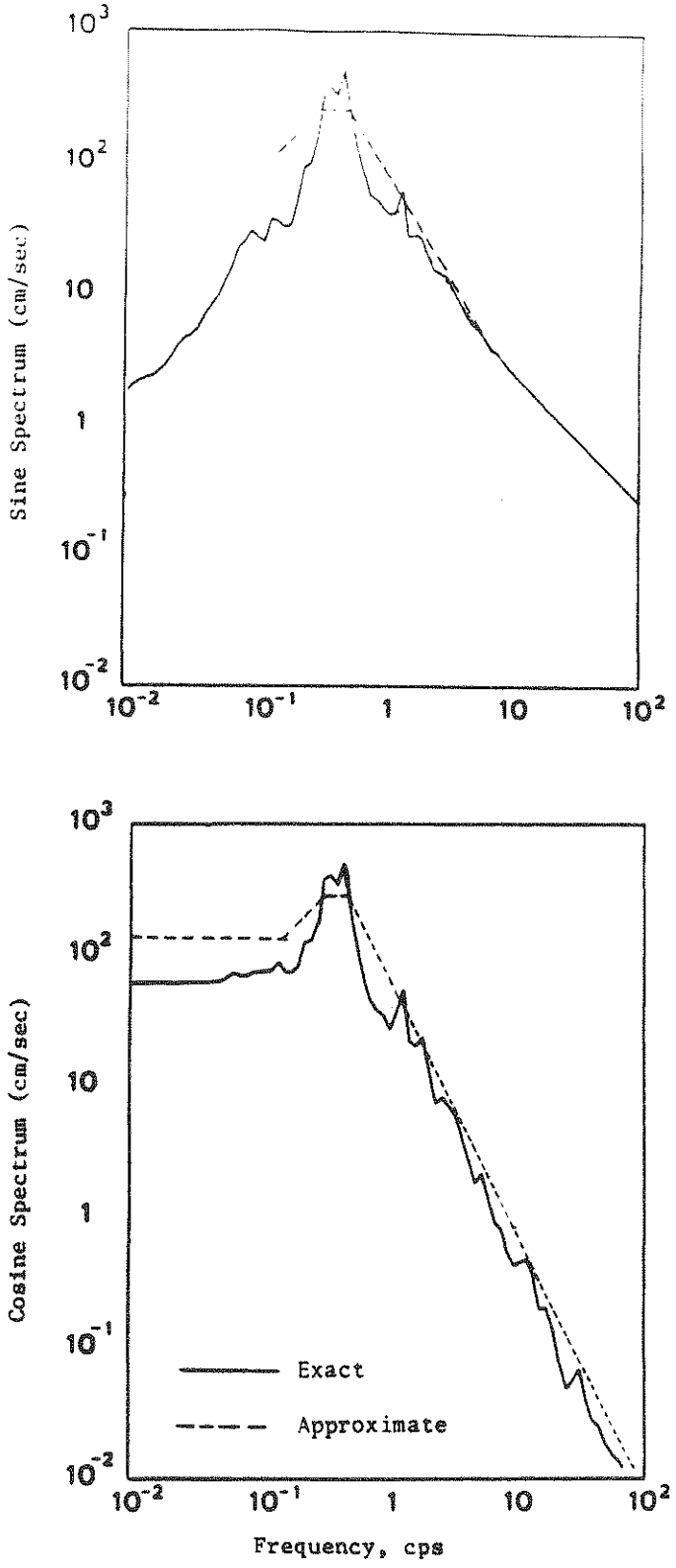

FIGURE 2f Sine and Cosine Spectra for Mexico City Earthquake, ξ = 20%

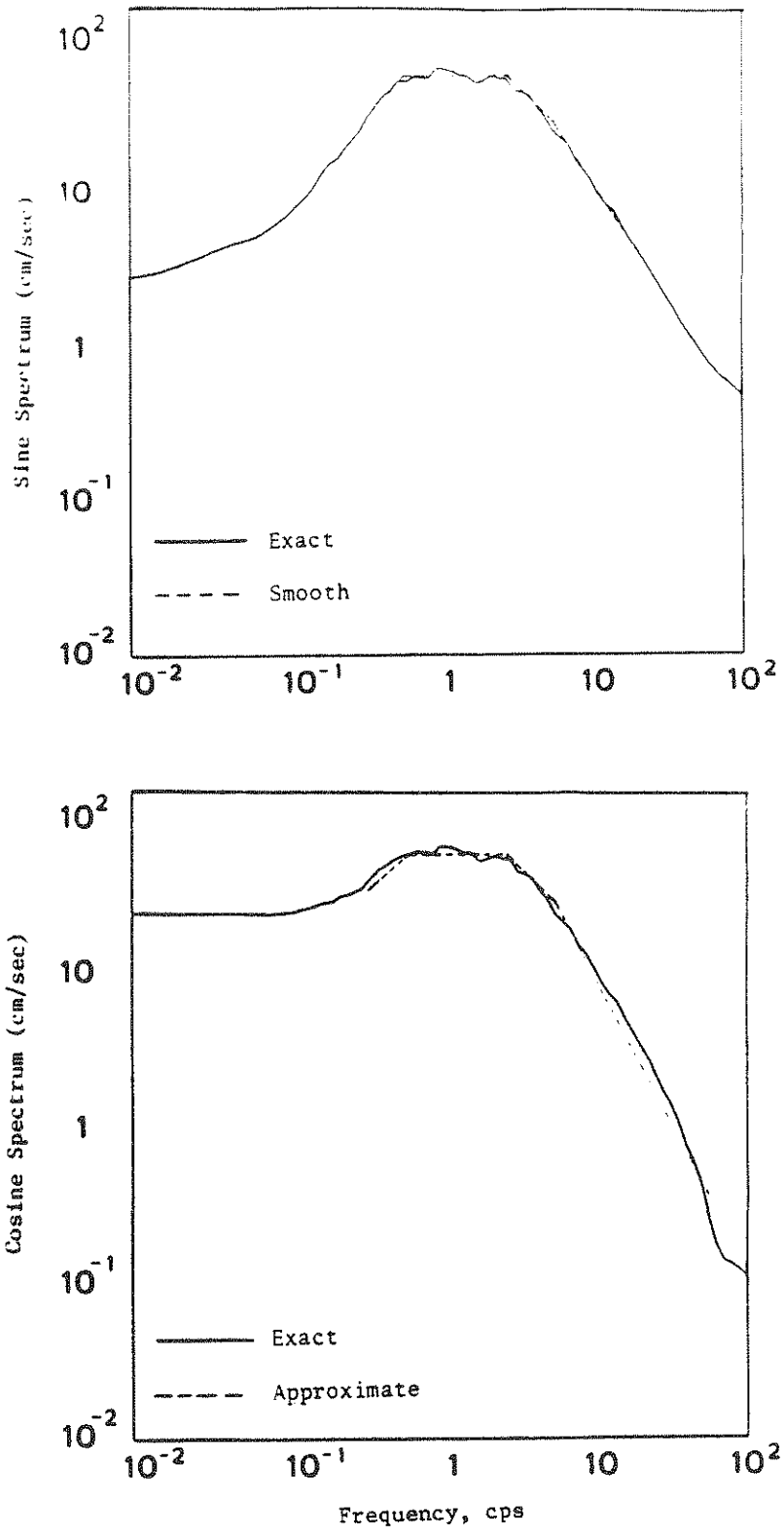

FIGURE 2g Average Sine and Cosine Spectra for Twenty Simulated Ground Accelerations, ξ = 2%

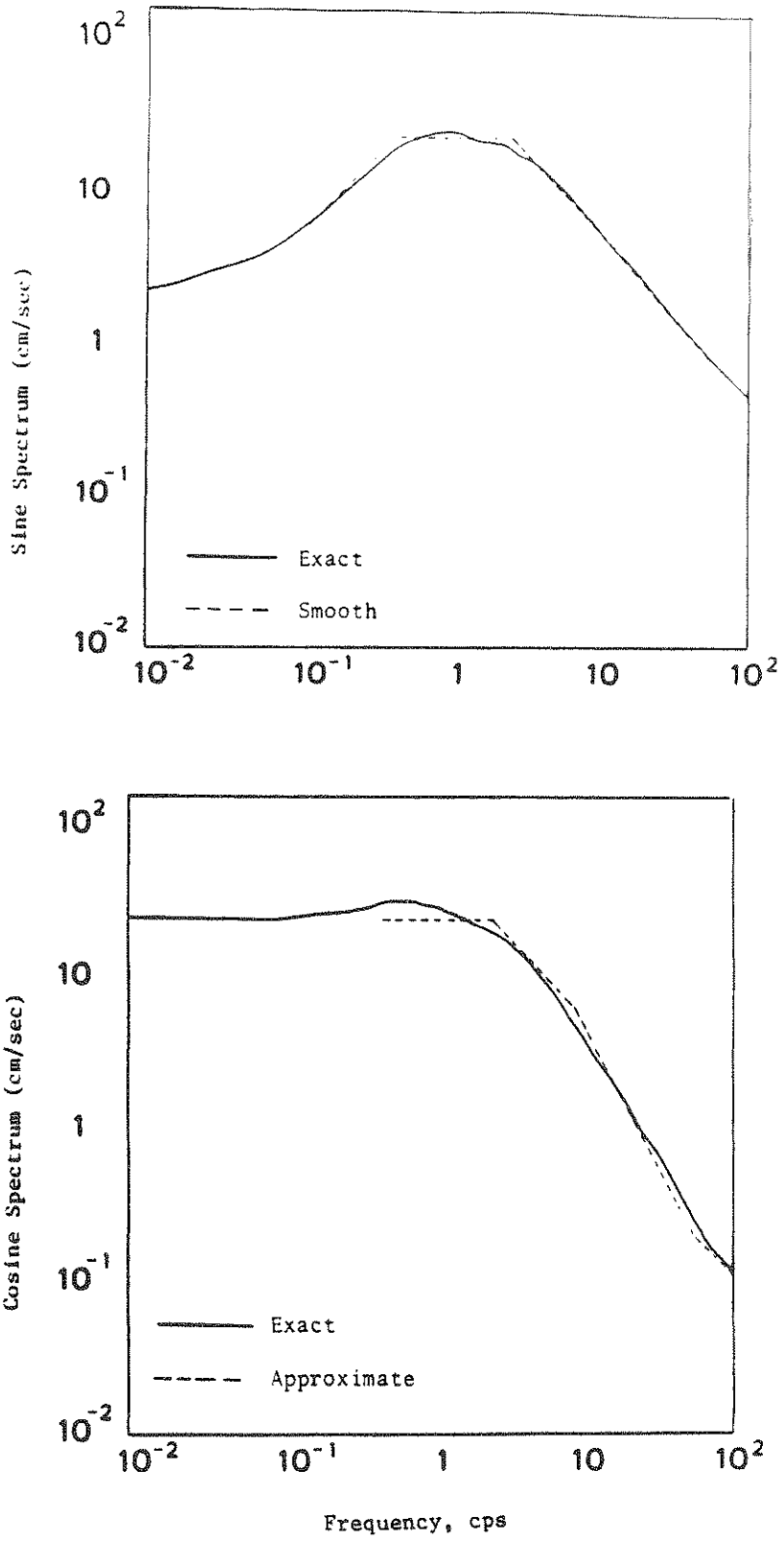

FIGURE 2h Average Sine and Cosine Spectra for Twenty Simulated Ground Accelerations, ξ = 20%

SECTION 5

COMBINING MAXIMUM MODAL RESPONSES

We are now in the position to obtain the approximate maximum structural response from the sine and cosine spectra. Recall that the vector of structural response $\underline{X}$ is given by Eq. (30), i.e.,

$$\underline{X} = \sum_{j=1}^{n} \left[\underline{\Gamma}_j \, S_j(t) + \underline{\Delta}_j \, C_j(t) \right] \tag{46}$$

The earthquake ground acceleration is modeled as a random process with zero mean. Further, it is assumed that the stationary segment of the ground acceleration is long compared with the period of the structure, so that the structural response can be considered as a stationary random process with zero mean. Thus, $S_j(t)$ and $C_j(t)$ are all stationary random processes with zero mean. The stationary variance of the structural response can be obtained from Eq. (46) as follows

$$\begin{aligned} \underline{\sigma}_{\underline{x}}^2 &= \sum_{i=1}^{n} \sum_{j=1}^{n} E\Big[\underline{\Gamma}_i \, \underline{\Gamma}_j \, S_i(t) \, S_j(t) + 2\underline{\Gamma}_j \, \underline{\Delta}_i \, S_j(t) \, C_i(t) \\ &\qquad + \underline{\Delta}_i \, \underline{\Delta}_j \, C_i(t) \, C_j(t) \Big] \\ &= \sum_{i=1}^{n} \sum_{j=1}^{n} \Big[\underline{\Gamma}_i \, \underline{\Gamma}_j \, \rho(S_i, S_j) \, \sigma_{S_i} \, \sigma_{S_j} + 2\underline{\Gamma}_j \, \underline{\Delta}_i \, \rho(S_j, C_i) \, \sigma_{S_j} \sigma_{C_i} \\ &\qquad + \underline{\Delta}_i \, \underline{\Delta}_j \, \rho(C_i, C_j) \, \sigma_{C_i} \sigma_{C_j} \Big] \end{aligned} \tag{47}$$

in which σ_{s_j} and σ_{c_j} are the standard deviations of $S_j(t)$ and $C_j(t)$, respectively, and $\rho(S_i, S_j) = E\left[S_i(t) \, S_j(t)\right] / \sigma_{s_i} \sigma_{s_j}$ is the correlation coefficiant of $S_i(t)$ and $S_j(t)$. Similar definition holds for the correlation coefficiants $\rho(C_i, C_j)$ and $\rho(S_i, C_j)$.

For a stationary random process with zero mean, such as $S_j(t)$ and $C_j(t)$, the mean of the maximum value may be expressed in approximation by a peak

factor γ multiplied by the standard deviation. Assuming that the peak factor γ for all stationary processes $C_j(t)$ and $S_j(t)$, for $j = 1,2,\ldots,n$, as well as the response vector process $\underline{X}(t)$ is identical, i.e., $\tilde{S}_j = \gamma\sigma_{s_j}$, $\tilde{C}_j = \gamma\,\sigma_{c_j}$ for $j = 1,2,\ldots,n$ and $\underline{X}_m = \text{maxi.}\ |\underline{X}(t)| = \gamma\ \underline{\sigma}_{\underline{X}}$, one obtains from Eq. (47) the square of the maximum response as follows

$$|\underline{X}_m^2| = \sum_{i=1}^{n}\sum_{j=1}^{n}\left[\underline{\Gamma}_i\ \underline{\Gamma}_j\ \rho(S_i,S_j)\ \tilde{S}_i\ \tilde{S}_j + 2\underline{\Gamma}_i\ \underline{\Delta}_j\ \rho(S_i,C_j)\ \tilde{S}_i\ \tilde{C}_j + \underline{\Delta}_i\ \underline{\Delta}_j\ \rho(S_i,C_j)\ \tilde{C}_i\ \tilde{C}_j\right] \tag{48}$$

in which the jth element of the vector $|\underline{X}_m^2|$ given above is the square of the maximum value of the relative displacement to the moving base of the jth floor.

For classically damped system, $\underline{\Delta}_j = 0$ and Eq. (48) reduces to the Complete Quadratic Combination (CQC) methed [13]. Since the sine and cosine spectra, $\tilde{S}_j$ and $\tilde{C}_j$, have been estimated previously, the remaining step is to evaluate the correlation coefficients in approximation. Der Kiureghian [3] computed the correlation coefficients $\rho(S_i,S_j)$ for the sine spectrum using the filtered white noise as the input excitation and compared with the corresponding results when the input excitation is white noise. His conclusion is that the correlation coefficients $\rho(S_i,S_j)$ under filtered white noise input can very well be approximated by that due to a white noise input when the damping is not very large (e.g. ξ<20%). Hence, the correlation coefficients $\rho(S_i,S_j)$ obtained using the white noise excitation can be used for the computation of the maximum response.

Here, we suggest the use of the white noise excitation as input to compute the correlation coefficients, $\rho(S_i,S_j)$, $\rho(S_i,C_j)$ and $\rho(C_i,C_j)$ appearing in Eq. (48). The results are given in the following (detailed

derivations are presented in the Appendix)

$$\rho(S_i,S_j) = 8a_{ij}\ c_{ij}\ \omega_i\omega_j/d_{ij} \tag{49a}$$

$$\rho(C_i,C_j) = 4a_{ij}\ b_{ij}\ c_{ij}/d_{ij}\left[(1+\xi_i^2)(1+\xi_j^2)\right]^{1/2} \tag{49b}$$

$$\rho(S_i,C_j) = 4a_{ij}\ \omega_i(b_{ij} - 2\omega_{Dj}^2)/d_{ij}(1+\xi_j^2)^{1/2} \tag{49c}$$

where

$$a_{ij} = (\xi_i\xi_j\omega_i\omega_j)^{1/2} \tag{50a}$$

$$b_{ij} = \omega_i^2 + \omega_j^2 + 2\xi_i\xi_j\omega_i\omega_j \tag{50b}$$

$$c_{ij} = \xi_i\omega_i + \xi_j\ \omega_j \tag{50c}$$

$$d_{ij} = b_{ij}^2 - 4\omega_{Di}^2\ \omega_{Dj}^2 \tag{50d}$$

SECTION 6

NUMERICAL EXAMPLES

In order to demonstrate the accuracy of the response spectrum approach developed in this paper, the maximum response of several nonclassically damped structural systems subjected to several earthquake ground excitations will be considered. Based on a detailed study conducted in Ref. 14, the effect of nonclassical damping is significant for certain primary-secondary systems subjected to earthquake excitations; particularly if the equipment is light and it is tuned to a frequency of the primary structure. Therefore, emphasis is placed on approximating the maximum response of several nonclassically damped primary-secondary systems.

All the example problems are subjected to the 1940 El Centro, 1971 San Fernando, 1985 Mexico City earthquakes, and simulated nonstationary ground accelerations described in Eqs. (33) and (34). The parameters that describe the envelope function, $\alpha(t)$, and the spectral density, $\phi_{\ddot{x}\ddot{x}}(\omega)$, of the earthquake modal are: $t_1 = 3$ sec., $t_2 = 13$ sec., $\beta = 0.26$, $\omega_g = 3.0$ Hz., $\xi_g = 0.65$, $\omega_0 = 0.5$ Hz., $\xi_0 = 0.71$ and $S^2 = 74.7 \times 10^{-4}$ $m^2/sec.^3/rad.$ With these parameters a simulated ground acceleration is shown in Fig. 3.

The maximum structural responses (i.e. story displacements and story deformations) are obtained using the following approaches.

1. The wilson-θ direct time history integration method. The maximum response thus obtained is exact, referred to as the exact solution.

2. The response spectrum approach proposed. Recall that this approach requires the knowledge of the sine spectrum (pseudo-velocity response spectrum) and cosine spectrum of the ground motion. The cosine spectrum may be generated from the time history of the ground acceleration (if available) or approximated from the sine spectrum using the guidelines discussed in section IV. For the example problems studied the

maximum response is obtained using both the excat and approximate cosine spectra.

3. The approximate classically damped approach. In this approach, the second order equations of motion are decoupled using egenvectors of the undamped system by disregarding the off-diagonal terms of the $\underline{\Phi}'\ \underline{C}\ \underline{\Phi}$ matrix, where $\underline{\Phi}$ is the (nxn) modal matrix of the undamped system. Then the maximum response is obtained from the sine spectrum using the SRSS procedure.

The above solutions are obtained for a particular earthquake, such as El Centro or simulated sample earthquake. Likewise, The maximum response of all the example problems were also computed using the average sine and cosine spectra for twenty simulated ground motions having the power spectral density and envelope function described previously. However for this situation one cannot obtain the exact maximum values of the response quantities. The maximum structural response obtained using various approaches will be compared to demonstrate the validity of each approach.

The first example problem consists of a two-degree-of-freedom shear beam type structure. This structure is classically damped if $C_1/k_1 = C_2/k_2$. The mass and stiffness of each story unit are: $m_1 = m_2 = m = 30$ tons and $k_1 = k_2 = k = 19{,}379$ kN/m. The natural frequencies of the structure are 2.5 Hz and 6.5 Hz, respectively.

Let values of C_1 and C_2 be equal to 123.4 kN/m/sec. so that the structure is classically damped with first modal damping ratio of 5%. Now the distribution of the damping is varied so the structure becomes nonclassically damped. Two nonclassically damped structures are considered. First all the damping of the structure is placed in the first story unit; with the results $C_1 = 246.8$ kN/m/sec. and $C_2 = 0.0$. Next all the damping of the structure is placed in the second story unit, leading to the results $C_1 = 0.0$ and $C_2 = 246.8$ kN/m/sec. Tables 1-a through 1-c presents the maximum story

deformations (U_1,U_2) of the structure with these three different damping distributions. An examination of the Table indicates that, as expected, the effect of nonclassical damping on this type of structural system is not significant and that either of the response spectrum procedures (i.e. classical or nonclassical damping) predicts maximum structural responses that are in close agreement with the exact solutions.

Next consider the classically damped two-story structure of example 1 in which a light single-degree-of-freedom equipment is mounted on the top floor. Such a primary structure is classically damped if $C_1/k_1 = C_2/k_2$ where $C_1 = C_2$ = 123.4 kN/m.sec. and the combined equipment-structure system is classically damped if $C_1/k_1 = C_2/k_2 = C_e/k_e$ where the subscript e referes to the equipment. In Ref. 14 it was shown that the effect of nonclassical damping for this equipment-structure system is significant if (i) the equipment is tuned to a frequency of the primary structure, (ii) the equipment mass is light compared to the tuned modal mass of the primary structure, and (iii) the equipment damping ratio is smaller than the damping ratio ξ_{ec} that results in a classically damped equipment-structure system.

Let the equipment frequency, ω_e, be tuned to the fundamental frequency of the primary structure, i.e. ω_e = 2.5 Hz. and the mass ratio (equipment mass over the first modal mass of the primary structure which is 30 tons) be equal to 10^{-4}. For this equipment-structure system the value of ξ_{ec} is equal to 5%. Tables 2-a through 2-c presents the maximum response of the equipment structure system for 3 different damping ratios of the equipment i.e. ξ_e = 0%, 5%, and 10%.

Examination of the results in Table 2-a, which correspond to ξ_e = 0%, indicates that the displacement of the equipment relative to the attachment point using the response spectrum approach developed in this paper is only 6% higher than the exact solution for the El Centro earthquake, 12% higher for

the San Fernando earthquake, 14% higher for the Mexico City earthquake, and 31% higher for the simulated earthquake. Whereas using the approximate classically damped approach, the response is 73% lower than the exact solution for the El Centro earthquake, 71% lower for the San Fernando earthquake, 25% lower for the Mexico City earthquake, and 60% lower for the simulated earthquake. A comparison of the results obtained using the approximate cosine spectra with those obtained using the exact cosine spectra for various earthquakes considered except the Mexico City indicates excellent agreement. For Mexico City earthquake the maximum equipment response using the approximate cosine spectra is 46% lower than that using the exact cosine spectra. As expected, the effect of nonclassical damping on the response of the primary structure is insignificant and the maximum responses obtained using different approaches are in close agreement. Results obtained using the response spectrum of a single ground acceleration record and those obtained using the average response spectrum of twenty records exhibit similar trends.

Table 2-b presents the maximum response when the equipment- structure system is classically damped (i.e. $\xi_e=\xi_{ec}=5\%$). Of course for this situation the nonclassically damped response spectrum approach reduces to classically damped response spectrum prodecure and these results are in good agreement with the exact solutions.

Table 2-c presents the results when the equipment damping ratio is 10%. Examination of the equipment displacement relative to the attachment point indicates that the equipment response using the response spectrum approach developed is again in good agreement with the exact solutions. The maximum deformation of the equipment is within 21% of the exact solution for all four earthquakes. However, the equipment response is 250% higher than the exact solution when the approximate classically damped approach is used. The results obtained using approximate cosine spectra are in remarkable agreement

with those using the exact cosine spectra for all earthquakes. Again, for the simulated earthquakes the results obtained using one and twenty sample records exhibit similar trends.

Next we examine the response of the equipment mounted on top of the two nonclassically damped structures of example 1. Again the equipment is tuned to the fundamental frequency of the primary structure and three different damping ratios for the equipment are considered (i.e. ξ_e = 0%, 5% and 10%). Tables 3-a through 3-c present the maximum story deformation for the equipment-structure system in which all the dampings of the primary structure are placed in the lower story unit. The corresponding results for the case in which all the dampings of the primary structure are placed in the second story unit are presented in Tables 4-a through 4-c.

It is observed from these tables that the maximum equipment deformation based on the response spectrum approach developed in this paper is within 44% of the exact solutions. However, based on the approximate classically damped procedure the equipment responses deviate up to 490% of the exact solutions. On the other hand, the effect of nonclassical damping on the primary structure response is insignifant. The results obtained using the approximate cosine spectra are very close to those obtained from exact cosine spectra.

Suppose the equipment is detuned and its frequency is chosen to be the average of the first two natural frequencies of the primary structure. Similar to the tuned equipment-structure system, three different damping distributions for the primary structure are considered and the equipment is undamped, i.e., ξ_e=0. Tables 5-a through 5-c present the response of the detuned equipment-structure system. It is observed from these tables that the accuracy for the proposed response spectrum approach, is well within 40%, whereas the accuracy for the approximate classically damped procedure is within 71% of the exact solution. Furthermore, the results obtained using

exact and approximate cosine spectra are very close. Finally, the response due to one simulated earthquake or twenty samples of simulated earthquakes exhibits similar trends.

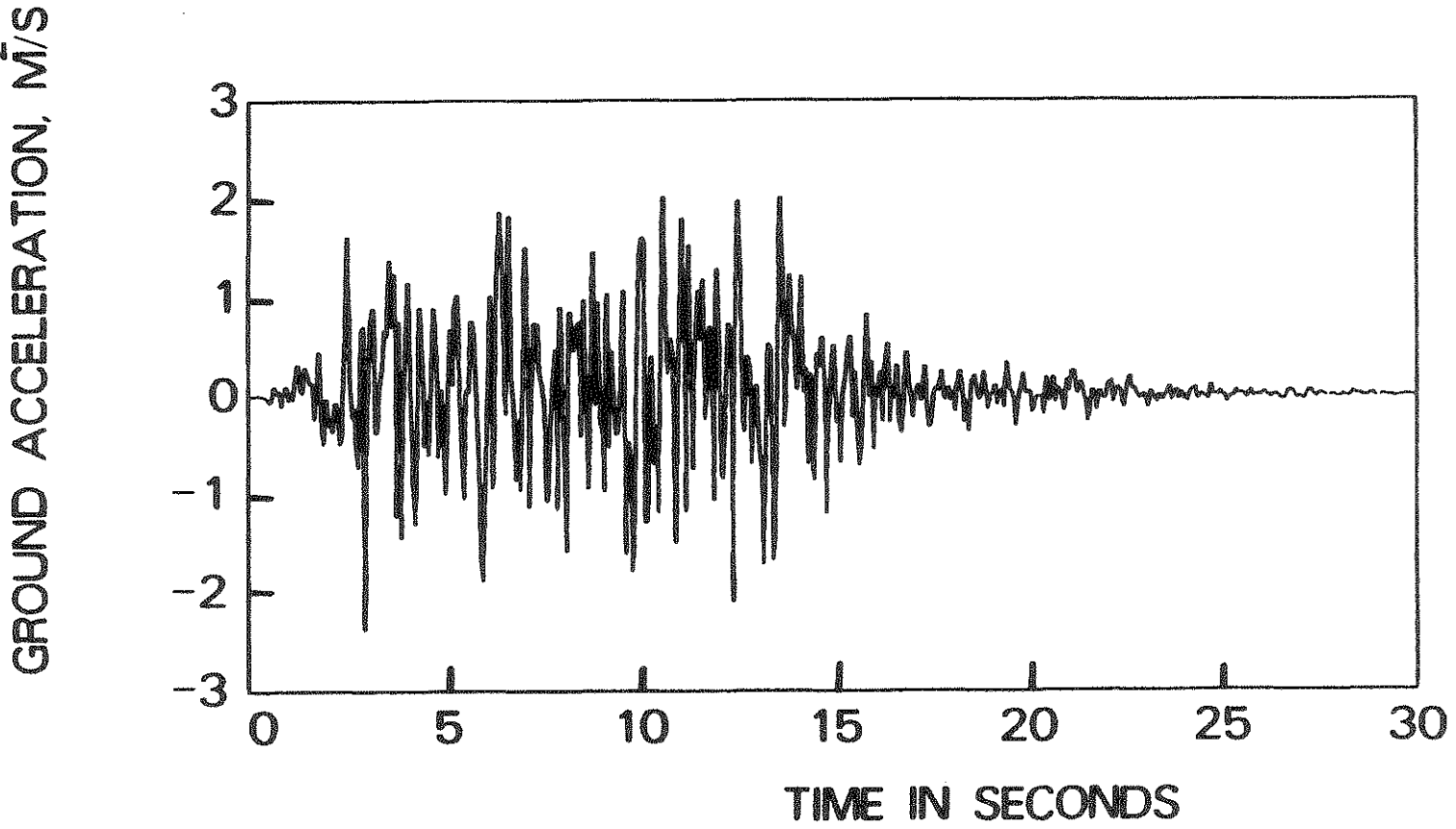

FIGURE 3 Simulated Ground Acceleration

TABLE 1: MAXIMUM RESPONSE OF TWO-DEGREE-OF-FREEDOM STRUCTURE (CM.)

(a) $C_1 = C_2 = 123.4$ kN/m.sec.

	El Centro		San Fernando		Mexico City		Simulated (1 sample)		Simulated (20-sample)	
	U_1	U_2	U_1	U_2	U_1	U_2	U_1	U_2	U_1	U_2
(1)	1.76	1.09	1.89	1.17	0.61	0.38	1.43	0.89	1.84	1.14
(2)	1.76	1.09	1.89	1.17	0.61	0.38	1.43	0.89	1.84	1.14
(3)	1.76	1.09	1.89	1.17	0.61	0.38	1.43	0.89	1.84	1.14
(4)	1.80	1.05	1.87	1.20	0.64	0.34	1.44	0.86	-	-

(b) $C_1 = 246.8$ kN/m.sec., $C_2 = 0$

(1)	1.54	0.97	1.69	1.06	0.58	0.36	1.16	0.75	1.55	0.98
(2)	1.54	0.97	1.69	1.06	0.58	0.36	1.16	0.74	1.55	0.98
(3)	1.53	0.95	1.67	1.03	0.57	0.36	1.16	0.73	1.54	0.96
(4)	1.61	0.98	1.67	1.11	0.60	0.32	1.15	0.77	-	-

(c) $C_1 = 246.8$ kN/m.sec., $C_2 = 0$

(1)	2.24	1.35	2.32	1.40	0.70	0.42	2.00	1.20	2.40	1.45
(2)	2.24	1.35	2.32	1.40	0.70	0.42	2.00	1.21	2.40	1.45
(3)	2.12	1.31	2.21	1.36	0.68	0.42	1.98	1.22	2.34	1.45
(4)	2.25	1.30	2.32	1.39	0.72	0.38	2.01	1.19	-	-

(1) Exact Cosine Spectrum; (2) Approximate Cosine Spectrum;
(3) Approximate Classically Damped Approach; (4) Exact Solution

TABLE 2. MAXIMUM DEFORMATION OF TUNED EQUIPMENT-STRUCTURE SYSTEM (CM.)

($\omega_e = \omega_1$, $C_1 = C_2 = 123.4$ kN/m/sec.)

(a) $\xi_e = 0\%$

	El Centro			San Fernando			Mexico City			Simulated (1 sample)			Simulated (20-sample)		
	U_1	U_2	U_e	U_1	U_2	U_e	U_1	U_2	U_e	U_1	U_2	U_e	U_1	U_2	U_e
(1)	1.78	1.10	76.96	1.90	1.18	84.48	0.61	0.38	10.76	1.44	0.90	53.62	1.85	1.14	70.62
(2)	1.78	1.10	77.68	1.90	1.18	84.84	0.62	0.38	5.84	1.44	0.90	55.61	1.85	1.14	70.65
(3)	1.76	1.09	20.09	1.89	1.17	21.70	0.61	0.38	7.03	1.43	0.88	16.37	1.98	1.12	25.94
(4)	1.79	1.05	72.43	1.89	1.20	75.70	0.64	0.34	9.44	1.43	0.85	40.78	-	-	-

(b) $\xi_e = 5\%$

(1)	1.76	1.09	20.03	1.90	1.17	21.73	0.61	0.38	7.04	1.43	0.88	16.61	1.83	1.13	21.07
(2)	1.76	1.09	20.03	1.90	1.17	21.73	0.61	0.38	7.04	1.42	0.88	16.61	1.83	1.13	21.07
(3)	1.76	1.09	20.03	1.90	1.17	21.73	0.61	0.38	7.04	1.42	0.88	16.58	1.92	1.19	22.05
(4)	1.80	1.05	14.42	1.87	1.20	17.90	0.64	0.34	5.78	1.44	0.85	15.53	-	-	-

(c) $\xi_e = 10\%$

(1)	1.76	1.09	8.97	1.89	1.17	11.30	0.61	0.38	1.58	1.43	0.89	7.86	1.84	1.13	11.69
(2)	1.76	1.09	10.75	1.89	1.17	11.84	0.61	0.38	1.52	1.43	0.88	8.95	1.84	1.13	12.12
(3)	1.75	1.08	20.06	1.89	1.17	21.86	0.61	0.38	7.07	1.42	0.88	17.00	1.91	1.18	22.66
(4)	1.80	1.05	9.15	1.87	1.20	10.87	0.64	0.34	2.00	1.44	0.86	9.66	-	-	-

(1) Exact Cosine Spectrum; (2) Approximate Cosine Spectrum;

(3) Approximate Classically Damped Approach; (4) Exact Solution

TABLE 3. MAXIMUM DEFORMATION OF TUNED EQUIPMENT-STRUCTURE SYSTEM (CM.)

($\omega_e = \omega_1$, $C_1 = 246.8$ kN/m/sec., $C_2 = 0.0$)

(a) $\xi_e = 0\%$

	El Centro			San Fernando			Mexico City			Simulated (1 sample)			Simulated (20-sample)		
	U_1	U_2	U_e	U_1	U_2	U_e	U_1	U_2	U_e	U_1	U_2	U_e	U_1	U_2	U_e
(1)	1.55	0.98	56.25	1.69	1.07	60.50	0.58	0.36	7.80	1.16	0.75	38.05	1.55	0.98	49.68
(2)	1.70	1.07	60.67	1.70	1.07	60.68	0.58	0.36	4.30	1.16	0.75	38.79	1.55	0.98	49.63
(3)	1.54	0.95	12.29	1.67	1.03	13.19	0.57	0.36	4.57	1.15	0.73	9.20	1.73	1.08	17.71
(4)	1.61	0.98	54.17	1.67	1.41	57.97	0.60	0.32	6.89	1.14	0.77	29.94	-	-	-
							(b) $\xi_e = 5\%$								
(1)	1.54	0.97	11.53	1.69	1.06	14.15	0.58	0.36	2.47	1.15	0.74	10.28	1.55	0.98	15.45
(2)	1.54	0.97	14.08	1.69	1.07	14.55	0.58	0.36	2.44	1.15	0.74	13.59	1.55	0.98	15.98
(3)	1.53	0.95	12.39	1.67	1.03	13.17	0.57	0.36	4.57	1.15	0.73	9.22	1.68	1.04	13.63
(4)	1.61	0.98	11.79	1.67	1.11	14.38	0.60	0.32	2.33	1.15	0.77	12.17	-	-	-
							(c) $\xi_e = 10\%$								
(1)	1.54	0.97	8.04	1.69	1.06	9.98	0.58	0.36	1.33	1.16	0.75	6.99	1.54	0.98	9.34
(2)	1.54	0.97	8.70	1.69	1.06	10.65	0.58	0.36	1.38	1.16	0.75	5.99	1.55	0.98	9.64
(3)	1.53	0.95	12.58	1.67	1.03	13.26	0.57	0.36	4.58	1.15	0.76	9.29	1.65	1.03	13.67
(4)	1.61	0.98	7.59	1.67	1.11	8.43	0.60	0.32	1.71	1.15	0.77	7.69	-	-	-

(1) Exact Cosine Spectrum; (2) Approximate Cosine Spectrum;

(3) Approximate Classically Damped Approach; (4) Exact Solution

TABLE 4. MAXIMUM DEFORMATION OF TUNED EQUIPMENT-STRUCTURE SYSTEM (CM.)

($\omega_e = \omega_1$, $C_1 = 0.0$, $C_2 = 246.8$ kN/m/sec.)

(a) $\xi_e = 0\%$

	El Centro			San Fernando			Mexico City			Simulated (1 sample)			Simulated (20-sample)		
	U_1	U_2	U_e	U_1	U_2	U_e	U_1	U_2	U_e	U_1	U_2	U_e	U_1	U_2	U_e
(1)	2.28	1.38	132.91	2.36	1.43	147.20	0.71	0.43	18.64	2.04	1.23	97.70	2.45	1.48	128.09
(2)	2.29	1.38	133.53	2.36	1.43	147.95	0.71	0.43	14.91	2.05	1.24	102.90	2.45	1.48	128.13
(3)	2.11	1.30	44.96	2.20	1.36	46.00	0.68	0.42	14.01	1.96	1.21	40.73	2.00	1.19	67.80
(4)	2.24	1.30	122.10	2.31	1.38	140.35	0.72	0.39	16.08	2.00	1.19	67.84	-	-	-
							(b) $\xi_e = 5\%$								
(1)	2.24	1.35	21.79	2.31	1.39	26.42	0.71	0.43	3.86	1.99	1.20	22.28	2.39	1.45	16.49
(2)	2.24	1.35	26.55	2.31	1.39	26.30	0.71	0.43	3.45	1.99	1.20	25.90	2.39	1.44	29.00
(3)	2.11	1.30	44.40	2.20	1.36	45.51	0.68	0.42	13.98	1.96	1.21	41.04	2.34	1.44	49.86
(4)	2.24	1.30	26.10	2.31	1.38	25.98	0.72	0.39	3.28	2.01	1.19	21.12	-	-	-
							(c) $\xi_e = 10\%$								
(1)	2.24	1.35	12.37	2.31	1.40	15.24	0.70	0.42	2.10	1.99	1.20	11.96	2.39	1.45	29.15
(2)	2.24	1.35	15.02	2.31	1.40	15.45	0.70	0.42	1.81	1.99	1.20	13.95	2.39	1.44	16.66
(3)	2.11	1.30	44.12	2.20	1.36	44.54	0.68	0.42	14.03	1.96	1.21	41.71	2.35	1.45	49.00
(4)	2.25	1.30	12.84	2.32	1.39	14.49	0.72	0.38	2.38	2.01	1.19	12.79	-	-	-

(1) Exact Cosine Spectrum; (2) Approximate Cosine Spectrum;

(3) Approximate Classically Damped Approach; (4) Exact Solution

TABLE 5. MAXIMUM DEFORMATION OF TUNED EQUIPMENT-STRUCTURE SYSTEM (CM.)

($\omega_e = (\omega_1 + \omega_2)/2$, $\xi_e = 0\%$)

(a) $C_1 = C_2 = 123.4$ kN/m/sec.

	El Centro			San Fernando			Mexico City			Simulated (1 sample)			Simulated (20-sample)		
	U_1	U_2	U_e	U_1	U_2	U_e	U_1	U_2	U_e	U_1	U_2	U_e	U_1	U_2	U_e
(1)	1.76	1.09	2.42	1.89	1.17	2.10	0.61	0.38	0.55	1.43	0.88	3.38	1.84	1.14	2.60
(2)	1.76	1.09	2.42	1.89	1.17	2.10	0.61	0.38	0.54	1.43	0.88	3.38	1.84	1.13	2.60
(3)	1.76	1.09	1.42	1.89	1.17	1.55	0.61	0.38	0.47	1.43	0.89	1.40	1.84	1.13	1.58
(4)	1.76	1.13	2.38	1.87	1.20	2.48	0.64	0.34	0.40	1.44	0.86	3.54	-	-	-
	(b) $C_1 = 2c = 246.8$ kN/m/sec., $C_2 = 0.0$														
(1)	1.54	0.97	2.51	1.69	1.06	2.13	0.58	0.36	0.54	1.16	0.75	3.61	1.55	0.98	2.69
(2)	1.54	0.97	2.51	1.69	1.06	2.14	0.58	1.39	0.54	1.16	0.75	3.61	1.55	0.98	2.70
(3)	1.53	0.95	1.26	1.67	1.03	1.32	0.57	0.36	0.44	1.15	0.73	1.09	1.54	0.96	1.27
(4)	1.61	0.98	2.63	1.67	1.11	2.69	0.60	0.32	0.39	1.15	0.77	3.73	-	-	-
	(c) $C_1 = 0.0$, $C_2 = 246.8$ kN/m/sec.														
(1)	2.24	1.35	2.61	2.32	1.40	2.30	0.70	0.42	0.60	2.00	1.20	3.51	2.40	1.45	2.81
(2)	2.24	1.35	2.61	2.32	1.40	2.30	0.70	0.42	0.60	2.00	1.21	3.51	2.40	1.45	2.81
(3)	2.13	1.31	1.86	2.21	1.36	2.03	0.68	0.42	0.55	1.98	1.22	2.71	2.34	1.45	2.42
(4)	2.25	1.30	2.63	2.32	1.39	2.71	0.72	0.38	0.43	2.01	1.19	3.65	-	-	-

(1) Exact Cosine Spectrum; (2) Approximate Cosine Spectrum;
(3) Approximate Classically Damped Approach; (4) Exact Solution

SECTION 7

CONCLUSIONS

A response spectrum approach for the seismic analysis of non- classically damped structural systems has been presented. Similar to the response spectrum approach for analysis of classically damped structures, the only information required for the ground motion input is the response spectrum. The maximum response of the nonclassically damped structure is expressed in terms of the sine spectrum and the cosine spectrum. The sine spectrum is directly related to the response spectrum of the ground acceleration, whereas the cosine spectrum is obtained in approximation from the response spectrum as well. The formulation takes into account the effect of cross correlation of modes with closely spaced frequencies.

The proposed approach has been applied to approximate the maximum response of several nonclassically damped structural systems subjected to several earthquake ground accelerations. Particular emphasis is placed on evaluating the maximum response of structural systems in which the effect of nonclassical damping is known to be significant.

Numerical results are compared with the exact solutions obtained by numerically integrating the equations of motion. It is shown that the accuracy of the proposed approach is quite reasonable. Also presented are maximum response quantities obtained using the approximate classically damped solutions. Numerical results indicate that the accuracy of proposed approach is generally better than that of the approximate classically damped solutions.

SECTION 8

REFERENCES

1. Caughey, T.H., and O'Kelly, E.J., "Classical Normal Modes in Damped Linear Dynamic Systems," Journal of Applied Mechanics, ASME 32, 583-588, 1985.

2. Clough, R.W., and Penzien, J., "Dynamics of Structures," McGraw Hill, New York, 1975.

3. Der Kiureghian, A., "A response Spectrum Approach for Random Vibrations," Report No. UCB/EERC-80/15, Earthquake Engineering Research Center, University of California, Berkeley, California, 1980.

4. Foss, K.A., "Coordinates Which Uncouples the Equations of Motion of Damped Linear Dynamic Systems," Journal of Applied Mechanics, ASME 25, 361-364, 1958.

5. Gupta, A.K. and Jaw, J.W., "Response Spectrum Method for Non-classically Damped Systems," Nuclear Engineering and Design, Vol. 91, pp.161-169.

6. Igusa, T. and Der Kiureghian, A., "Dynamic Analysis of Multiply Tuned and Arbitrarily Supported Secondary Systems," Report No. UCB/EERC-83/07, University of California, Berkeley, July 1983.

7. Kanai, K., "Semi-Empirical Formula for Seismic Characterization of The Ground," Bulletin of Earthquake Research Institute, University of Tokyo, Japan, Vol. 35, June 1967.

8. Newmark, N.M., Blume, J.A., and Kapur, K.K.," Seismic Design Spectra for Nuclear Power Plants," Journal of the Power Division, ASCE, Vol. 99, 1973, pp. 287-303.

9. Singh, M.P., "Seismic Response by SRSS for Proportional Damping," Journal of the Engineering Mechanics Division, ASCE, Vol. 106, 1980, pp. 1405-1419.

10. Traill-Nash, R.W., "Modal Methods in the Dynamics of Systems with Nonclassical Damping," Earthquake Engineering and Structural Dynamics, Vol. 9, 153-169, 1983.

11. Veletsos, A.S., and Ventura, C.E., "Modal Analysis of Non-classically Damped Linear Systems," Earthquake Engineering and Structural Dynamics, Vol. 14, 217-243, 1986.

12. Villaverde, R. and Newmark, N.M., "Seismic Response of Light Attachments to Buildings," SRS No. 469, Univ. of Illinois, Feb. 1980.

13. Wilson, E.L., Der Kiureghian, A. and Bayo, E.P.," A Replacement for the SRSS Method in Seismic Analysis," Earthquake Engineering and Structural Dynamics, Vol. 9, 187-194, 1981.

14. Yang, J.N., Sarkani, S. and Long, F.X., "Modal Analysis of Non-classicially Damped Structural Systems Using Canonical Transformation," National Center For Earthquake Engineering Research, Technical Report No. NCEER-87-0019, September 1987, SUNY, Buffalo, N.Y.

APPENDIX

CALCULATION OF CORRELATION COEFFICIENTS

In this Appendix, the various correlation coefficients needed to compute the approximate maximum response will be evaluated. These correlation coefficients are defined as

$$\rho(S_i,S_j) = E(S_iS_j)/\sigma_{S_i}\,\sigma_{S_j} \tag{I.1a}$$

$$\rho(C_i,C_j) = E(C_iC_j)/\sigma_{C_i}\,\sigma_{C_j} \tag{I.1b}$$

$$\rho(S_i,C_j) = E(S_iC_j)/\sigma_{S_i}\,\sigma_{C_j} \tag{I.1c}$$

in which

$$E(S_iS_j) = E\Big[\int_0^t\int_0^t e^{-\xi_i\omega_i\tau_1}\sin\omega_{Di}\tau_1\;\ddot{x}_g(t-\tau_1)\;e^{-\xi_j\omega_j\tau_2}\sin\omega_{Dj}\tau_2\;\ddot{x}_g(t-\tau_2)\;d\tau_1,d\tau_2\Big] \tag{I.2}$$

Similary $E(C_iC_j)$ is given by Eq. (I.2) with $\sin\omega_{Di}\tau_1$ and $\sin\omega_{Dj}\tau_2$ being replaced by $\cos\omega_{Di}\tau_1$ and $\cos\omega_{Dj}\tau_2$, respectively, and $E(S_iC_j)$ is also given by Eq. (I-2) with $\sin\omega_{Dj}\tau_2$ being replaced by $\cos\omega_{Di}\tau_2$.

With the assumption that the eqrthquake ground acceleration $\ddot{x}_g(t)$ is a stationary white noise with zero mean and a power spectral density S_0, Eq. (I.2) can be obtained as follows.

$$E(S_iS_j) = E\Big[\int_0^\infty\int_0^\infty \ddot{x}_g(t-\tau_1)\;e^{-\xi_i\omega_i\tau_1}\sin\omega_{Di}\tau_1\;d\tau_1\;\ddot{x}_g(t-\tau_2)\;e^{-\xi_j\omega_j\tau_2}\sin\omega_{Dj}\tau_2\;d\tau_2\Big]$$

$$= \int_0^\infty \int_0^\infty E\left[\ddot{x}_g(t-\tau_1)\ \ddot{x}_g(t-\tau_2)\right] e^{-\xi_i\omega_i\tau_1} \sin \omega_{Di}\tau_1\, d\tau_1$$

$$e^{-\xi_j\omega_j\tau_2} \sin \omega_{Dj}\tau_2\, d\tau_2$$

$$= \int_0^\infty \int_0^\infty R_{\ddot{x}\ddot{x}}(\tau_1-\tau_2)\, e^{-\xi_i\omega_i\tau_1} \sin \omega_{Di}\tau_1\, d\tau_1\, e^{-\xi_j\omega_j\tau_2} \sin \omega_{Dj}\tau_2\, d\tau_2$$

$$= \int_0^\infty 2\pi S_0\, e^{-\xi_i\omega_i\tau_2} \sin \omega_{Di}\tau_2\, e^{-\xi_j\omega_j\tau_2} \sin \omega_{Dj}\tau_2\, d\tau_2$$

$$= \pi S_0 \left[\frac{\xi_i \omega_i + \xi_j \omega_j}{(\xi_i \omega_i + \xi_j \omega_j)^2 + (\omega_{Di} - \omega_{Dj})^2}\right.$$

$$\left. - \frac{\xi_i \omega_i + \xi_j \omega_j}{(\xi_i \omega_i + \xi_j \omega_j)^2 + (\omega_{Di} + \omega_{Dj})^2}\right]$$

$$= \frac{\pi S_0 (\xi_i\omega_i + \xi_j\omega_j)(4\omega_{Di}\omega_{Dj})}{(\omega_i^2 + \omega_j^2 + 2\xi_i\xi_j\omega_i\omega_j)^2 - 4\omega_{Di}^2\omega_{Dj}^2} \qquad \text{(I.3a)}$$

Similarly, the expressions for $E(C_iC_j)$ and $E(S_iC_j)$ can be obtained as follows

$$E(C_iC_j) = \pi S_0 \left[\frac{\xi_i \omega_i + \xi_j \omega_j}{(\xi_i \omega_i + \xi_j \omega_j)^2 + (\omega_{Di} - \omega_{Dj})^2}\right.$$

$$\left. + \frac{\xi_i \omega_i + \xi_j \omega_j}{(\xi_i \omega_i + \xi_j \omega_j)^2 + (\omega_{Di} + \omega_{Dj})^2}\right]$$

$$= \frac{\pi S_0(\xi_i\omega_i + \xi_j\omega_j)(2\omega_i^2+2\omega_j^2 + 4\xi_i\xi_j\omega_i\omega_j)}{(\omega_i^2 + \omega_j^2 + 2\xi_i\xi_j\omega_i\omega_j)^2 - 4\omega_{Di}^2\omega_{Dj}^2} \qquad \text{(I.3b)}$$

and

$$E(S_i C_j) = \pi S_0 \left[\frac{\omega_{Di} + \omega_{Dj}}{(\xi_i \omega_i + \xi_j \omega_j)^2 + (\omega_{Di} + \omega_{Dj})^2} + \frac{\omega_{Di} - \omega_{Dj}}{(\xi_i \omega_i + \xi_j \omega_j)^2 + (\omega_{Di} - \omega_{Dj})^2} \right]$$

$$= \frac{\pi S_0 (2\omega_{Di})(\omega_i^2 + \omega_j^2 + 2\xi_i \xi_j \omega_i \omega_j + 2\omega_{Dj}^2)}{(\omega_i^2 + \omega_j^2 + 2\xi_i \xi_j \omega_i \omega_j)^2 - 4\omega_{Di}^2 \omega_{Dj}^2} \qquad \text{(I.3c)}$$

The mean square values are obtained by setting indicies i and j equal to each other in Eqs. (I.3a) and (I.3b) as follows

$$E(S_i^2) = \sigma_{S_i}^2 = \frac{\pi S_0 (1-\xi_i^2)}{2\xi_i \omega_i} \qquad \text{(I.4a)}$$

$$E(C_i^2) = \sigma_{C_i}^2 = \frac{\pi S_0 (1+\xi_i^2)}{2\xi_i \omega_i} \qquad \text{(I.4b)}$$

Substituting Eqs. (I.3) and (I.4) into Eqs. (I.1), one obtains the three correlation coefficients in the following

$$\rho(S_i, S_j) = 8a_{ij} c_{ij} \omega_i \omega_j)/d_{ij} \qquad \text{(I.5a)}$$

$$\rho(C_i, C_j) = 4a_{ij} b_{ij} c_{ij}/d_{ij} \left[(1+\xi_i^2)(1+\xi_j^2) \right]^{1/2} \qquad \text{(I.5b)}$$

$$\rho(S_i, C_j) = 4a_{ij} \omega_i (b_{ij} - 2\omega_{Dj}^2)/d_{ij} (1+\xi_j^2)^{1/2} \qquad \text{(I.5c)}$$

and

$$a_{ij} = (\xi_i \xi_j \omega_i \omega_j)^{1/2} \qquad \text{(I.6a)}$$

$$b_{ij} = \omega_i^2 + \omega_j^2 + 2\xi_i \xi_j \omega_i \omega_j \qquad \text{(I.6b)}$$

$$c_{ij} = \xi_i \omega_i + \xi_j \omega_j \qquad \text{(I.6c)}$$

$$d_{ij} = b_{ij}^2 - 4\omega_{Di}^2 \omega_{Dj}^2 \qquad \text{(I.6d)}$$

NATIONAL CENTER FOR EARTHQUAKE ENGINEERING RESEARCH
LIST OF PUBLISHED TECHNICAL REPORTS

The National Center for Earthquake Engineering Research (NCEER) publishes technical reports on a variety of subjects related to earthquake engineering written by authors funded through NCEER. These reports are available from both NCEER's Publications Department and the National Technical Information Service (NTIS). Requests for reports should be directed to the Publications Department, National Center for Earthquake Engineering Research, State University of New York at Buffalo, Red Jacket Quadrangle, Buffalo, New York 14261. Reports can also be requested through NTIS, 5285 Port Royal Road, Springfield, Virginia 22161. NTIS accession numbers are shown in parenthesis, if available.

NCEER-87-0001 "First-Year Program in Research, Education and Technology Transfer," 3/5/87, (PB88-134275/AS).

NCEER-87-0002 "Experimental Evaluation of Instantaneous Optimal Algorithms for Structural Control," by R.C. Lin, T.T. Soong and A.M. Reinhorn, 4/20/87, (PB88-134341/AS).

NCEER-87-0003 "Experimentation Using the Earthquake Simulation Facilities at University at Buffalo," by A.M. Reinhorn and R.L. Ketter, to be published.

NCEER-87-0004 "The System Characteristics and Performance of a Shaking Table," by J.S. Hwang, K.C. Chang and G.C. Lee, 6/1/87, (PB88-134259/AS).

NCEER-87-0005 "A Finite Element Formulation for Nonlinear Viscoplastic Material Using a Q Model," by O. Gyebi and G. Dasgupta, 11/2/87, (PB88-213764/AS).

NCEER-87-0006 "Symbolic Manipulation Program (SMP) - Algebraic Codes for Two and Three Dimensional Finite Element Formulations," by X. Lee and G. Dasgupta, 11/9/87, (PB88-219522/AS).

NCEER-87-0007 "Instantaneous Optimal Control Laws for Tall Buildings Under Seismic Excitations," by J.N. Yang, A. Akbarpour and P. Ghaemmaghami, 6/10/87, (PB88-134333/AS).

NCEER-87-0008 "IDARC: Inelastic Damage Analysis of Reinforced Concrete-Frame Shear-Wall Structures," by Y.J. Park, A.M. Reinhorn and S.K. Kunnath, 7/20/87, (PB88-134325/AS).

NCEER-87-0009 "Liquefaction Potential for New York State: A Preliminary Report on Sites in Manhattan and Buffalo," by M. Budhu, V. Vijayakumar, R.F. Giese and L. Baumgras, 8/31/87, (PB88-163704/AS).

NCEER-87-0010 "Vertical and Torsional Vibration of Foundations in Inhomogeneous Media," by A.S. Veletsos and K.W. Dotson, 6/1/87, (PB88-134291/AS).

NCEER-87-0011 "Seismic Probabilistic Risk Assessment and Seismic Margin Studies for Nuclear Power Plants," by Howard H.M. Hwang, 6/15/87, (PB88-134267/AS).

NCEER-87-0012 "Parametric Studies of Frequency Response of Secondary Systems Under Ground-Acceleration Excitations," by Y. Yong and Y.K. Lin, 6/10/87, (PB88-134309/AS).

NCEER-87-0013 "Frequency Response of Secondary Systems Under Seismic Excitations," by J.A. HoLung, J. Cai and Y.K. Lin, 7/31/87, (PB88-134317/AS).

NCEER-87-0014 "Modelling Earthquake Ground Motions in Seismically Active Regions Using Parametric Time Series Methods," G.W. Ellis and A.S. Cakmak, 8/25/87, (PB88-134283/AS).

NCEER-87-0015 "Detection and Assessment of Seismic Structural Damage," by E. DiPasquale and A.S. Cakmak, 8/25/87, (PB88-163712/AS).

NCEER-87-0016 "Pipeline Experiment at Parkfield, California," by J. Isenberg and E. Richardson, 9/15/87, (PB88-163720/AS).

NCEER-87-0017 "Digital Simulations of Seismic Ground Motion," by M. Shinozuka, G. Deodatis and T. Harada, 8/31/87, (PB88-155197/AS).

NCEER-87-0018 "Practical Considerations for Structural Control: System Uncertainty, System Time Delay and Truncation of Small Forces," J. Yang and A. Akbarpour, 8/10/87, (PB88-163738/AS).

NCEER-87-0019 "Modal Analysis of Nonclassically Damped Structural Systems Using Canonical Transformation," by J.N. Yang, S. Sarkani and F.X. Long, 9/27/87, (PB88-187851/AS).

NCEER-87-0020 "A Nonstationary Solution in Random Vibration Theory," by J.R. Red-Horse and P.D. Spanos, 11/3/87, (PB88-163746/AS).

NCEER-87-0021 "Horizontal Impedances for Radially Inhomogeneous Viscoelastic Soil Layers," by A.S. Veletsos and K.W. Dotson, 10/15/87, (PB88-150859/AS).

NCEER-87-0022 "Seismic Damage Assessment of Reinforced Concrete Members," by Y.S. Chung, C. Meyer and M. Shinozuka, 10/9/87, (PB88-150867/AS).

NCEER-87-0023 "Active Structural Control in Civil Engineering," by T.T. Soong, 11/11/87, (PB88-187778/AS).

NCEER-87-0024 "Vertical and Torsional Impedances for Radially Inhomogeneous Viscoelastic Soil Layers," by K.W. Dotson and A.S. Veletsos, 12/87, (PB88-187786/AS).

NCEER-87-0025 "Proceedings from the Symposium on Seismic Hazards, Ground Motions, Soil-Liquefaction and Engineering Practice in Eastern North America, October 20-22, 1987, edited by K.H. Jacob, 12/87, (PB88-188115/AS).

NCEER-87-0026 "Report on the Whittier-Narrows, California, Earthquake of October 1, 1987," by J. Pantelic and A. Reinhorn, 11/87, (PB88-187752/AS).

NCEER-87-0027 "Design of a Modular Program for Transient Nonlinear Analysis of Large 3-D Building Structures," by S. Srivastav and J.F. Abel, 12/30/87, (PB88-187950/AS).

NCEER-87-0028 "Second-Year Program in Research, Education and Technology Transfer," 3/8/88, (PB88-219480/AS).

NCEER-88-0001 "Workshop on Seismic Computer Analysis and Design With Interactive Graphics," by J.F. Abel and C.H. Conley, 1/18/88, (PB88-187760/AS).

NCEER-88-0002 "Optimal Control of Nonlinear Structures," J.N. Yang, F.X. Long and D. Wong, 1/22/88, (PB88-213772/AS).

NCEER-88-0003 "Substructuring Techniques in the Time Domain for Primary-Secondary Structural Systems," by G. D. Manolis and G. Juhn, 2/10/88, (PB88-213780/AS).

NCEER-88-0004 "Iterative Seismic Analysis of Primary-Secondary Systems," by A. Singhal, L.D. Lutes and P. Spanos, 2/23/88, (PB88-213798/AS).

NCEER-88-0005 "Stochastic Finite Element Expansion for Random Media," P. D. Spanos and R. Ghanem, 3/14/88, (PB88-213806/AS).

NCEER-88-0006 "Combining Structural Optimization and Structural Control," F. Y. Cheng and C. P. Pantelides, 1/10/88, (PB88-213814/AS).

NCEER-88-0007 "Seismic Performance Assessment of Code-Designed Structures," H.H-M. Hwang, J. Jaw and H. Shau, 3/20/88, (PB88-219423/AS).

NCEER-88-0008 "Reliability Analysis of Code-Designed Structures Under Natural Hazards," H.H-M. Hwang, H. Ushiba and M. Shinozuka, 2/29/88.

NCEER-88-0009 "Seismic Fragility Analysis of Shear Wall Structures," J-W Jaw and H.H-M. Hwang, 4/30/88.

NCEER-88-0010 "Base Isolation of a Multi-Story Building Under a Harmonic Ground Motion - A Comparison of Performances of Various Systems," F-G Fan, G. Ahmadi and I.G. Tadjbakhsh, to be published.

NCEER-88-0011 "Seismic Floor Response Spectra for a Combined System by Green's Functions," F.M. Lavelle, L.A. Bergman and P.D. Spanos, 5/1/88.

NCEER-88-0012 "A New Solution Technique for Randomly Excited Hysteretic Structures," G.Q. Cai and Y.K. Lin, 5/16/88.

NCEER-88-0013 "A Study of Radiation Damping and Soil-Structure Interaction Effects in the Centrifuge," K. Weissman, supervised by J.H. Prevost, 5/24/88, to be published.

NCEER-88-0014 "Parameter Identification and Implementation of a Kinematic Plasticity Model for Frictional Soils," J.H. Prevost and D.V. Griffiths, to be published.

NCEER-88-0015 "Two- and Three-Dimensional Dynamic Finite Element Analyses of the Long Valley Dam," D.V. Griffiths and J.H. Prevost, to be published.

NCEER-88-0016 "Damage Assessment of Reinforced Concrete Structures in Eastern United States," A.M. Reinhorn, M.J. Seidel, S.K. Kunnath and Y.J. Park, 6/15/88.

NCEER-88-0017 "Dynamic Compliance of Vertically Loaded Strip Foundations in Multilayered Viscoelastic Soils," S. Ahmad and A.S.M. Israil, 6/17/88.

NCEER-88-0018 "An Experimental Study of Seismic Structural Response With Added Viscoelastic Dampers," R.C. Lin, Z. Liang, T.T. Soong and R.H. Zhang, 6/30/88, to be published.

NCEER-88-0019 "Experimental Investigation of Primary - Secondary System Interaction," G.D. Manolis, G. Juhn and A.M. Reinhorn, 5/27/88, to be published.

NCEER-88-0020 "A Response Spectrum Approach For Analysis of Nonclassically Damped Structures," J.N. Yang, S. Sarkani and F.X. Long, 4/22/88.

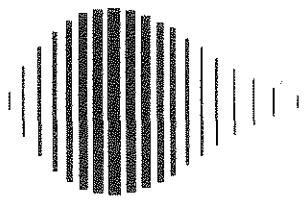

National Center for Earthquake Engineering Research
State University of New York at Buffalo